AFCRL-62-378

First Annual Report

"On the Propagation of VLF Waves in Solids"

Dr. Wolfram Bitterlich

Contract no. 61(052)-490 December 1961

C O N T E N T S

Summary

A theoretical and practical investigation of the propagation of electromagnetic waves of very low frequency in conducting rock was carried out under consideration of ε, μ, and $\varkappa$. In the course of these investigations it appeared that the decrease of the magnetic field strength strongly depends on the conductivity $\varkappa$ of the rock. The experimental results were largely corroborated by theoretical calculations. The parameters ε and μ have either been taken from tables or have been determined by sample measurements. As the majority of measurements was conducted in mine galleries it was necessary to develop special instruments for this purpose.

Introduction

Under contract with the United States Government work on the VLF research project was started in December 1960. The investigations were directed towards a study of the propagation of extremely long electromagnetic waves in solid and liquid media, the frequencies to be used being in the range from a few cycles to below 100 kc.

As the scope of this program is rather wide, the target for the first year was limited to the study of the propagation of a comparatively narrow low-frequency band in solids. In order to realize this project it became necessary from the outset to organize two collaborator groups: one group dealing with the mathematics and theoretical physics involved in the problem and another team engaging in the experimental and electronic work. The experimental team had as its objective the development and construction of the necessary apparatus, as transmitting and receiving equipment, special antennas etc. This team was also designated to measure the field strength of low frequency electromagnetic fields in rock. These measurements were conducted in mine workings in the vicinity of Innsbruck. Apart from this, it was required to develop and construct special equipment for measuring the electric data of mountain-building rock. The aim of the theoretical team was the mathematical elaboration of antenna problems of a fundamental nature. It was, for instance, of interest to determine whether electric or magnetic dipoles would yield better results in a con-

ducting medium. This program was extended by calculations on the propagation of magnetic fields in conducting rock under special consideration of ε, μ, and $\varkappa$.

In the present annual report are laid down the results obtained by both groups. Compared with the wide scope of the entire program this report is necessarily only of an initiatory nature; many problems remain as yet to be solved.

On this occasion I would like to express my gratitude and that of my collaborators for the generous financial support extended by the American authorities to this scientific research program. It was only owing to this help that it was feasible to initiate this wide range project which requires large material expenditures.

I am also deeply indebted to Univ. Prof. Dr. Steinmaurer for giving his permission to conduct part of the work within the Institute of Physics of the Innsbruck University.

I am also grateful to Univ. Prof. Dr. Gröbner and Univ. Prof. Dr. Cap for their valuable collaboration. I also wish to acknowledge the generous openmindedness of Director Dipl. Ing. G. Keitner of the "Montanwerke", Brixlegg, who granted permission to work in the mines of Schwaz and St. Gertraudi and also supported it. I am also thankful to the Works Managers Dipl. Ing. Klaker and Schwarz for their active help in the underground work.

I would also like to thank all my collaborators for their unceasing and successful scientific work during this year.

Persons engaged in work on the VLF Project:

Project Supervisor and Contractor: Dr. W. Bitterlich.

Experimental team:

O. Gröbner, graduate student
W. Gradl, technical assistant
O. Hörz, laboratory assistant
T. Elster, laboratory assistant

Theoretical team:

Univ. Prof. Dr. Gröbner (Mathematics)
Univ. Prof. Dr. Cap (Theoretical Physics)
Dr. R. Hommel
H. Oberhammer, graduate student

1. Theoretical Section

1,1. Theoretical Foundations of the Propagation of VLF Waves

Investigation of the propagation of electromagnetic waves of extremely large wavelength (VLF) in conducting media.

In the sequel it is endeavoured to study the behavior of the magnetic field in a medium characterized by the conductivity $\varkappa$, the dielectric constant ε, and the permeability μ as described by the complete set of MAXWELL's equations. First of all it is assumed that the three material parameters be considered constant, e. g., that they are independent of the frequency. This implies a certain simplification as regards the quantities ε and $\varkappa$, as these usually exhibit a frequency dependence varying greatly from one substance to another, as will be shown later. This dependence can be demonstrated taking ice as an example:

Frequency		$ohm^{-1}.m^{-1}$
260 kc	2.05	40.10^{-4}
4.6 c	153	1.10^{-4}

As the experimental investigations were limited to a relatively narrow frequency band, the above assumption is reasonably justified.

MAXWELL's equations are written down as follows:

$$\operatorname{curl} \vec{H} = \varepsilon \varepsilon_0 \dot{\vec{E}} + \varkappa \vec{E} \; ; \qquad \operatorname{div} \vec{E} = 0$$

$$\operatorname{curl} \vec{E} = -\mu \mu_0 \dot{\vec{H}} \; ; \qquad \operatorname{div} \vec{H} = 0$$

As has been explained above, ε, μ, and $\varkappa$ are assumed constant. By elimination of $\vec{E}$ the following equation results:

$$\nabla^2 \vec{H} = \varepsilon \varepsilon_0 \mu \mu_0 \ddot{\vec{H}} + \varkappa \mu \mu_0 \dot{\vec{H}} \qquad (2)$$

If $\vec{H} = \vec{A} . e^{i\omega t}$, there follows

$$\nabla^2 \vec{A} + k^2 \vec{A} = 0 \qquad (3)$$

where $k^2 = \varepsilon \varepsilon_0 \mu \mu_0 \omega^2 \left(1 - \frac{i \varkappa}{\varepsilon \varepsilon_0 \omega}\right)$

k is a complex quantity of the form $k = k_1 + ik_2$.
It is found to be

$$k_{1/2} = \omega \sqrt{\varepsilon \varepsilon_0 \mu \mu_0} \left[\sqrt{\tfrac{1}{2}\left(1 + \sqrt{1 + \left(\frac{\varkappa}{\varepsilon \varepsilon_0 \omega}\right)^2}\right)} - i \sqrt{\tfrac{1}{2}\left(-1 + \sqrt{1 + \left(\frac{\varkappa}{\varepsilon \varepsilon_0 \omega}\right)^2}\right)} \right] \qquad (4)$$

In order to be in a position to solve equation (3) in the usual manner and to match our line of progress to the special problem at hand, spherical coordinates are introduced in the following:

$$x = r . \cos\varphi . \sin\vartheta \qquad 0 \leq r < \infty$$
$$y = r . \sin\varphi . \sin\vartheta \qquad 0 \leq \varphi \leq 2\pi$$
$$z = r . \cos\vartheta \qquad 0 \leq \vartheta \leq \pi$$

The components of H remain unchanged: H_x, H_y, and H_z.

If the Laplace operator is written in spherical coordinates and then introduced in equation (3), it assumes the form

$$\frac{\partial^2}{\partial r^2} + \frac{1}{r^2 \sin^2\vartheta} \frac{\partial^2}{\partial \varphi^2} + \frac{1}{r^2} \frac{\partial^2}{\partial \vartheta^2} + \frac{2}{r} \frac{\partial}{\partial r} + \frac{\cos\vartheta}{r^2 \sin\vartheta} \frac{\partial}{\partial \vartheta} + k^2 \vec{A} = 0 \qquad (5)$$

Equation (5) is now solved by the usual method of separating the variables: $\vec{A} = \vec{R}(r) . \vec{Y}(\varphi, \vartheta)$.

As is generally known, thereby two equations are obtained, the first of which depends only on r and the second only on φ and ϑ.

$$\text{(a):}\quad \vec{R}'' + \frac{2}{r}\vec{R}' + \left(k^2 - \frac{n(n+1)}{r^2}\right)\vec{R} = 0$$

$$\text{(b):}\quad \frac{1}{\sin^2\vartheta}\vec{Y}_{\varphi\varphi} + \vec{Y}_{\vartheta\vartheta} + \operatorname{cotg}\vartheta\,\vec{Y} + n(n+1)\vec{Y} = 0 \qquad (6)$$

where $n(n+1)$ is the separation constant.

Equation (6b) possesses solutions only for $n = 0, 1, 2, \ldots$. They are found to be the spherical harmonics $Y_n(\varphi, \vartheta)$, which can be represented as follows:

$$Y_n(\varphi,\vartheta) = \frac{\alpha_0}{2} P_n(\cos\vartheta) + \sum_{\nu=1}^{n} P_{n,\nu}(\cos\vartheta)\left[\alpha_\nu \cos\nu\varphi + \beta_\nu \sin\nu\varphi\right] \qquad (7)$$

for $n = 0, 1, 2, \ldots$.

In the course of the further investigations the dependence on φ and ϑ can be ignored, because the magnetic field strength has its largest value in the direction of the dipole axis, which circumstance is generally known. This special direction was observed in all measurements so that only the dependence upon r need be investigated in the measurements. It is described by equation (6a).

The further treatment of (6a) is rendered feasible by the substitution $x = kr$ and $R = x^{1/2}y$, by which (6a) is transformed into BESSEL's differential equation

$$y'' + \frac{1}{x}y' + \left(1 - \frac{(n+\frac{1}{2})}{x^2}\right)y = 0$$

This equation has for solutions the BESSEL functions with half-integral index

$$J_{(n+1/2)}(x) = C.\sqrt{x}.x^n \left(\frac{d}{xdx}\right)^n \begin{cases} \frac{\sin x}{x} \\ \frac{\cos x}{x} \end{cases} \qquad (7)$$

The desired function R_n can now be assembled as follows:

$$R_n = x^{-1/2} y(x) = x^n \left(\frac{d}{xdx}\right)^n \frac{C_1 \cdot \sin x + C_2 \cdot \cos x}{x}$$

By converting it back to the variable r one obtains

$$R_n(r) = r^n \left(\frac{d}{rdr}\right)^n \cdot \frac{e^{\pm ikr}}{r}$$

The field of a dipole is described with sufficient accuracy by the term of order 2 in the series expansion

$$R_2(r) = C \frac{1}{r} e^{ikr}\left(-k^2 - \frac{3ik}{r} + \frac{3}{r^2}\right)$$

where k is the complex quantity as specified above.

For an evaluation of the individual terms it is necessary to make the solution real. By setting $k = k_1 + ik_2$ one obtains by straightforwrad calculation the real solution of (6a)

$$R(r) = C \frac{e^{-k_2 r}}{r} \left(k_1^2 - k_2^2 - \frac{3k_2}{r} - \frac{3}{r^2}\right) \sin\left((t - t_o) + k_1 r\right) \cdot \left(2k_1 k_2 + \frac{3k_1}{r}\right) \cos\left((t - t_o) + k_1 r\right) \qquad (8)$$

This solution can be matched to our special problem by a suitable choice of the integration constants C and t_o.

Relation (8) presents a solution of the present problem insofar as it is correlated to the measurements conducted to date.

For the sake of completeness the solution of equation (2), the starting point of our investigation, is given below

$$|\vec{H}| = e^{i\omega t} R_2(r) Y_2(\varphi, \vartheta).$$

However, as the receiver was designed to detect only the modulus of $\bar{H}$, the following calculations proceed from the equation

$$\bar{H} = Q \frac{e^{-k_2 r}}{r} \sqrt{(k_1^2 - k_2^2 - \frac{3k_2}{r} - \frac{3}{r^2})^2 + (2k_1 k_2 - \frac{3}{r^2})^2} \quad (9)$$

In the evaluation of the expression (4) the following numerical data were used:

$$\mu_0 = 1.256.10^{-6} \left[\frac{Vsec}{A.m}\right] \qquad \mu = 1$$

$$\varepsilon_0 = \frac{10^7}{4\pi c^2} \left[\frac{Asec}{V.m}\right] \qquad \varepsilon = 10$$

$$\omega = 2\pi .10^4$$

For $\varkappa > 5.10^{-6}$ and in virtue of the values of the other constants

$$\frac{\varkappa}{\varepsilon\varepsilon_0\omega} \gg 1$$

and hence k can be evaluated as follows:

$$k_1 \sim k_2 \sim \sqrt{\frac{\varkappa\mu\mu_0\omega}{2}} = \frac{2\pi}{10}\sqrt{10\,\varkappa}$$

The quantity $\varkappa$ was used as a parameter in the subsequent calculations because it is just this quantity which experiences the most remarkable variations. The conductivities characteristic of the rock types encountered in this investigations varied from 10^{-4} to 10^{-3} $[ohm^{-1}m^{-1}]$.

In Fig. 1 the curves are illustrated that have been obtained for $\varkappa_1 = 10^{-5}$, $\varkappa_2 = 10^{-4}$, $\varkappa_3 = 5.10^{-4}$, and $\varkappa_4 = 10^{-3}$.

Formula (9) can be simplified if the magnitude of $\varkappa$ is taken into account. Assuming $\varkappa = 10^{-3}[ohm^{-1}m^{-1}]$, the relation

$$|\bar{B}| = C^* \frac{e^{-kr}}{r} 2k$$

holds from a distance of 20 m with sufficient accuracy.

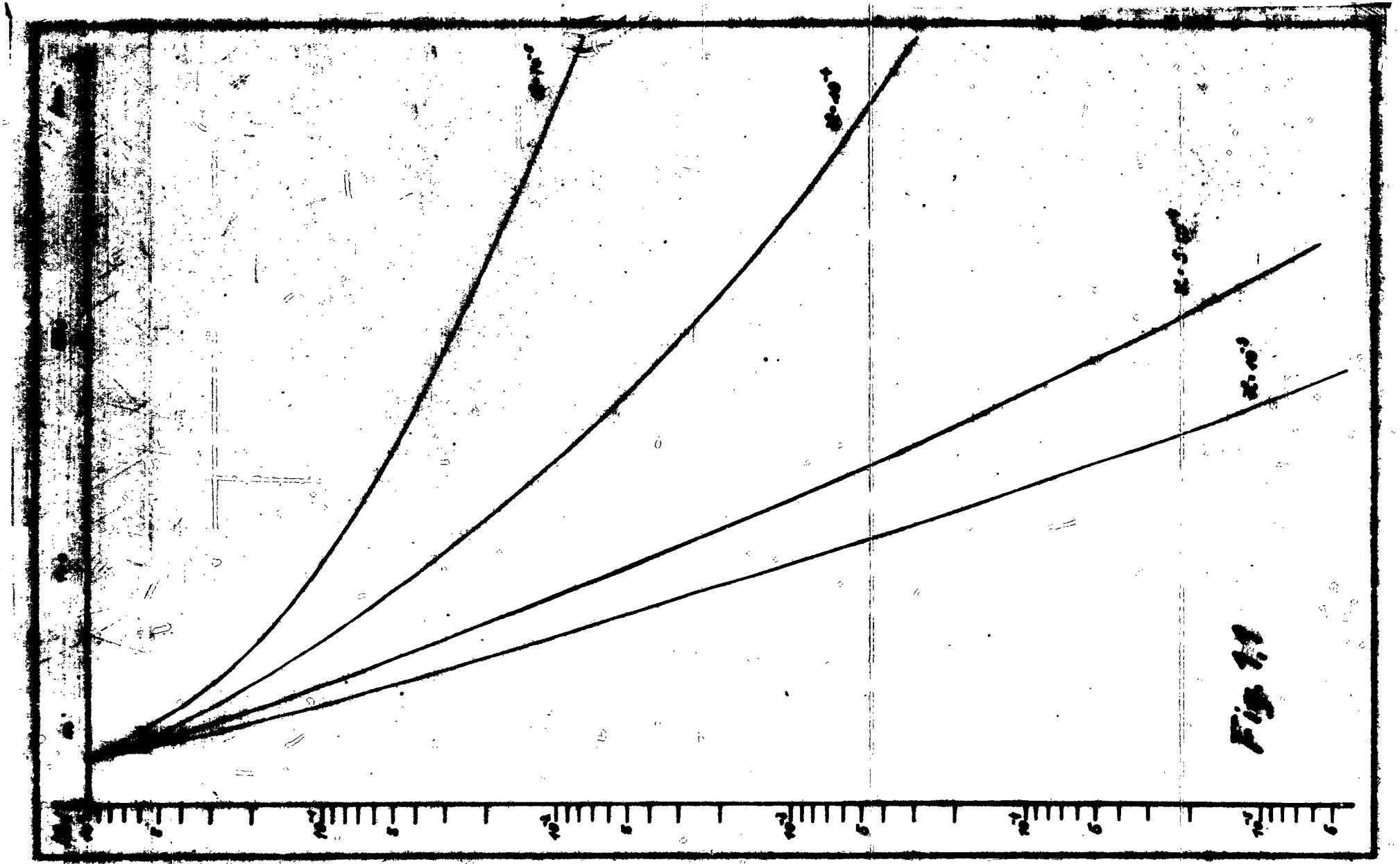

Fig. 11

1,2 Derivation of the Poynting Vector of an Electric and Magnetic Dipole

For extremely long electromagnetic waves the antenna forms that are practically realizable are described with sufficient accuracy by the equations of the elementary Hertzian dipole which, in dependence on the antenna current, read as follows:

Electric dipole:

$$E_r = \frac{2}{\varepsilon^* \varepsilon_0} \frac{J.dl}{4\pi i\omega}\left(\frac{1}{r^3} + \frac{ik^*}{r^2}\right) \cos\vartheta . e^{-ik^*r}$$

$$E_\vartheta = \frac{1}{\varepsilon^* \varepsilon_0} \frac{J.dl}{4\pi i\omega}\left(\frac{1}{r^3} + \frac{ik^*}{r^2} - \frac{k^{*2}}{r}\right) \sin\vartheta . e^{-ik^*r}$$

$$H_\varphi = \frac{J.dl}{4\pi}\left(\frac{1}{r^2} + \frac{ik^*}{r}\right) \sin\vartheta . e^{-ik^*r}$$

Magnetic dipole:

$$H_r = -\frac{2}{\mu\mu_0} \frac{\mu_0 JF}{4\pi}\left(\frac{1}{r^3} + \frac{ik^*}{r}\right) \cos\vartheta . e^{-ik^*r}$$

$$H_\vartheta = -\frac{1}{\mu\mu_0} \frac{\mu_0 JF}{4\pi}\left(\frac{1}{r^3} + \frac{ik^*}{r^2} - \frac{k^{*2}}{r}\right) \sin\vartheta . e^{-ik^*r}$$

$$E_\varphi = \frac{\mu_0 JFi\omega}{4\pi}\left(\frac{1}{r^2} + i\frac{k^*}{r}\right) \sin\vartheta . e^{-ik^*r}$$

Abandoning the possibility of increasing the antenna length dl or the antenna cross section F, the field strength realizable for a given frequency and distance is uniquely a function of the antenna current J which is, however, limited

(a) in the electric dipole: by the capacity attached at the end of the dipole and the antenna voltage,

(b) in the magnetic dipole: by the conductor losses in the frame and the transmitter power.

Moreover, the decision, what kind of dipole radiation is to be used with very long waves, depends on

(1) the radiation conditions in the vacuum
(2) the propagation conditions in the conducting medium
(3) which limitations, inherent to the apparatus and mentioned in item (a) and (b), can most easily be overcome.

(1) Radiation conditions in the vacuum:
It is known that the frequency characteristic of the radiation resistance of a magnetic dipole does not favor the emission of long waves. However, in this investigation stress was laid primarily on a maximum output of electric energy and not on a high antenna efficiency. From this viewpoint the magnetic-type antenna is more favorable than the capacitive dipole, because it permits the generation of higher field strengths, although at a lower efficiency.

If the electric field strength of a capacitive dipole with a length of 8 m, having a distributed capacity of 100 pF is calculated in a direction perpendicular to the dipole axis at a distance of 10 km, it attains the following value, the antenna voltage being 1000 V and the frequency 10 000 c:

$$E_{\vartheta} = \frac{8}{8.86.10^{-12}} \frac{1}{4\pi} 10^{-7} \left(\frac{1}{10^{12}} + i\frac{2\pi 10^{4}}{10^{8}.3.10^{8}} - \right.$$

$$\left. - \frac{4\pi^{2} 10^{4}}{9.10^{16}.10^{4}}\right) \sim 2.58.10^{-8} \quad [V/m]$$

Under otherwise equal conditions, a magnetic dipole as has been used in the measurements (cross section 0.8 m^2, conductor resistance 0.8 ohm, 40 turns) operated at a power level of 80 watts supplies a field strength

$$E_\varphi = \frac{1.25\cdot10^{-6}\cdot10\cdot40\cdot2\pi\cdot10^4}{4\pi}\left(\frac{1}{10^8} + i\frac{2\cdot10^4}{3\cdot10^8\cdot10^4}\right)$$

$$\sim 5.6\cdot10^{-8}\ [V/m]$$

It proceeds from these values that it is more easily realizable to produce appreciable field strengths by means of a magnetic dipole than by an electric one, in spite of the low efficiency of the former.

(2) Propagation conditions for the energy flux in a conducting medium:

As the experimental investigations were conducted underground, the conductivity of the surrounding rock had to be taken into account. For the sake of simplicity, the practical arrangement is simplified in the theoretical treatment: it was assumed that an empty sphere with radius r_0 ($\varepsilon, \mu = 1$, $\varkappa = 0$) is embedded in a uniform conducting material; the dipole is located at the center of the sphere. If both the electric and magnetic dipole are taken to radiate without loss, so that the power supplied to them is completely transformed into radiation energy and if the electric and magnetic dipole are supplied with N watts, we have on the surface of the sphere ($r = r_0$) $\overline{\sigma}_e = \overline{\sigma}_m$, that is

$$\mathrm{Re}\ E_\varphi \bar{H}_\varphi = \mathrm{Re}\ E_\varphi \bar{H}_\varphi$$

$$\mathrm{Re}\ \frac{m_e \bar{m}_e}{\varepsilon^* \varepsilon_0}\frac{1}{r_0^5} = -\mathrm{Re}\ \frac{m_m \bar{m}_m}{\mu\mu_0}\frac{\bar{k}^*(k^* - \bar{k}^*)}{r^3}$$

$$\mathrm{Re}\ \frac{1}{\varepsilon^*\varepsilon_0}\frac{m_e}{4\pi}\frac{1}{r_0^3}\frac{\bar{m}_e}{4\pi}i\omega\frac{1}{r_0^2} = -\mathrm{Re}\frac{1}{\mu\mu_0}\frac{m_m\,\bar{m}_m}{16\pi^2}i\omega \cdot \left(\frac{ik^*}{r^4} - \frac{i\bar{k}^*}{r^4} + \frac{\bar{k}^* k^*}{r^3} - \frac{\bar{k}^{*2}}{r^3}\right)$$

If the magnetic and electric dipole are to radiate the same amount of energy, the ratio of the dipole moments must be

$$\frac{m_e \bar{m}_e}{m_m \bar{m}_m} = -2r_o^2 \frac{\mathrm{Re}\, k\, J_m\, k}{j_m\, Z^2}$$

We will now investigate the energy density of both dipoles in the long-range field:

$$\overline{\sigma}_e = \frac{1}{2}\,\mathrm{Re}\,\frac{m_e \bar{m}_e\, j\omega}{\varepsilon^* \varepsilon_o 16\pi^2}\, j\,\frac{k^{*2}\bar{k}^*}{r^2}\, e^{-i(k^* - \bar{k}^*)r} \sin^2\vartheta;$$

$$\overline{\sigma}_m = \frac{1}{2}\,\mathrm{Re}\,\frac{m_m \bar{m}_m\, j\omega}{\mu\mu_o 16\pi^2}\,\frac{-i\bar{k}^{*2}\, k^*}{r^2}\, e^{-i(k^* - \bar{k}^*)r} \sin^2\vartheta.$$

Hence the ratio of the electric and magnetic energy density

$$\frac{\overline{\sigma}_e}{\overline{\sigma}_m} = \frac{m_e \bar{m}_e}{m_m \bar{m}_m}\,\frac{\mathrm{Re}\,\dfrac{k^*}{\varepsilon^* \varepsilon_o}}{-\mathrm{Re}\,\dfrac{\bar{k}^*}{\mu\mu_o}} = 2r_o^2\,\frac{J_m k^*\,\mathrm{Re}\, k^*\, Z^2}{J_m\, Z^2}$$

But $k^{*2} = \omega^2 \varepsilon_o \mu\mu_o \left(\varepsilon + \dfrac{\mathcal{H}}{i\omega\varepsilon_o}\right) = k_o^2 \varepsilon^*$;

$$Z = \sqrt{\frac{\mu\mu_o}{\varepsilon^*\varepsilon_o}} = \sqrt{\frac{\mu_o}{\varepsilon_o}}\,\frac{1}{\sqrt{\varepsilon}} = \frac{Z_o}{\sqrt{\varepsilon}}$$

and $u^* = \sqrt{\varepsilon^*}$,
and hence we have

$$\frac{\overline{\sigma}_e}{\overline{\sigma}_m} = 2r_o^2\,\frac{J_m k_o u^*\,\mathrm{Re}\, k_o u^*\, Z_o^2/u^{*2}}{J_m\, Z_o^2/u^{*2}}$$

$$= 8\pi^2 \left(\frac{r_o}{\lambda_o}\right)^2 \frac{J_m u^* + \mathrm{Re}\,(1/u^*)}{J_m\,(1/u^{*2})}$$

It can be easily taken from this relation that with

increasing wavelength, the value of $(r_o/\lambda_o)^2$ diminishes and hence the magnetic dipole becomes the more favorable transmitting antenna.

At a frequency of 10 kc, a sphere diameter of 1 m and a conductivity of 10^{-4} the ratio $\overline{\sigma_e}/\overline{\sigma_m} = 0.8 \cdot 10^{-5}$, both the magnetic and electric dipole radiating the same energy.

These considerations show that the magnetic dipole exhibits far more favorable properties than the electric one within the frequency range in question.

1,3 Magnetic Moment of an Air-core Coil.

It is desirable to have the magnetic moment as large as possible for a given transmitter power. This implies that according to the formula

$$M_m = n J F \mu_o$$

the current, the turns number and the antenna cross section should be made as large as possible. As, however, the requirements of a high turns number and antenna cross section are contradictory to a high antenna current (at given transmitter power), it is worthwile to investigate the question, which one of the design data has the most prominent influence on the magnetic moment. The following equations hold:

$$M_m = n J F \mu_o \; ; \quad J = (N/R)^{1/2} \; ; \quad R = \varrho l/q \; ;$$
$$F = r^2 \pi \; ; \quad l = 2r\pi n.$$

where ϱ = specific resistance, q = conductor cross section, l = length of wire, r = coil radius.

From these equations, the magnetic moment can be computed as follows:

$$M_m = nr^2\mu_o \ (Nq/\varrho l)^{1/2} = \frac{(Nq/\varrho)^{1/2}\ l^{3/2}}{4\pi n}$$

As can be easily seen from this formula, it is favorable to wind the given wire length in as few turns as possible. This means, however, that an antenna with large cross section performs better than one with many turns and a small cross section. The transmitting antennas SAIII and SAIV were designed in compliance with these considerations.

1,4 The Design of Transistorized Power Stages

The design of the new powerful transmitter was governed by the following considerations: if a transmitter having the limit impedance R_{lim} is opened up and blocked periodically by a sinusoidal voltage in class C operation, the internal resistance averaged over one full period is a function of the angle of flow of collector current:

$$R_i = R_{lim}/f_1$$

where

$$f_1 = \frac{\Theta - \frac{1}{2}\sin 2\Theta}{(1 - \cos\Theta)}$$

and

Θ = angle of flow of collector current.

The power supplied by the transistor is calculated from

$$N = \frac{1}{2} U_o^2 \frac{1}{R_{lim}} \frac{1}{(1 + \frac{1}{f_1 R_{a_1}/R_{lim}})(R_{a_1}/R_{lim} + \frac{1}{f_1})}$$

where U_o = battery voltage, R_{a_1} = load impedance.

The maximum output power depends on the angle of flow of collector current and on the ratio R_{a_1}/R_{lim}. It can be represented in a diagram from which can be taken the specific load impedance required for maximum output power at a given current. The efficiency is given by

$$\eta = \frac{1}{2} \frac{f_1^2}{f_o} \frac{1}{f_1 + \frac{1}{R_{a_1}/R_{lim}}}$$

where

$$f_o = \frac{1}{\pi} \frac{\sin\Theta - \cos\Theta}{1 - \cos\Theta}$$

The available power $N_\sim$ is, as is the case for the efficiency, a function of the two parameters Θ and R_{a_1}/R_{lim}, both of which can be chosen at liberty as design parameters. As $N_\sim$ and η depend on these parameters in a different manner, it is impossible to design simultaneously for optimum efficiency and maximum power output. Only one of these objectives is realizable at one time. At maximum output power

$$N_{\sim\, opt} = \frac{U_o^2}{8} \frac{f_1(\Theta)}{R_{lim}}$$

the efficiency is low, because for equal generator and load impedance it is natural that a large portion of the energy supplied is lost in the generator. If the design is intended to give high power output it is worthwile to investigate to what extent the maximum permissible collector dissipation permits an optimum design. The normalized collector dissipation is given by

$$\frac{Q}{U_o^2/R_{lim}} = \frac{f_o/f_1 \left(1 + \frac{1}{f_1 R_{a_1}/R_{lim}}\right) - \frac{1}{2}}{\left(1 + \frac{1}{f_1 R_{a_1}/R_{lim}}\right)\left(R_{a_1}/R_{lim} + \frac{1}{f_1}\right)}$$

If a diagram is constructed from the correlated values of Θ and R_{lim}, the constant collector dissipation being used as parameter, in which the output power is plotted against the impedance ratio, the optimum adjustment can be read from the diagram, for a given collector dissipation not to be exceeded.

Owing to the low limit impedance of transistors the voltage gain is very high, whence the following relationship between the three limit values Q, U_o, and I_{Cmax} results:

$$Q = (f_o - 0.45 f_1)\, U_o\, I_{Cmax}$$

If the power output is normalized to $N/I_{Cmax}U_o$, the relation

$$\frac{N}{I_{Cmax}U_o} = f_o(\Theta) - \frac{Q}{I_{Cmax}U_o}$$

holds. Hence it is only necessary to determine the maximum output power in dependence on Q: assuming an arbitrary value of Q, $(f_o - 0.45 f_1)$ is determined, whence the angle of flow of collector current, f_o, and the normalized output power are derived successively. The optimum output power is obtained, if the collector dissipation, the maximum collector current and the maximum collector voltage are correlated as follows:

$$Q = 0.18\, I_{Cmax}U_o$$

In the next stage of work investigations are planned in which the transistor is driven by rectangular pulses.

2. Experimental Section

2,1 P r e p a r a t o r y W o r k

The experimental work envisaged within the VLF project is mostly in a frequency range which to date has seen very few measurements of a comparable nature. Hence it was endeavoured to use higher frequencies (below 200 kc), in particular in the early stages of the work. This enabled us to include findings in our comparison which were, for instance, obtained by FRITSCH in the Schwaz mine about ten years ago. FRITSCH made measurements in the short- and long range region to bridge underground distances as large as possible. He also had in mind the utilization of his experiments for the establishment of communication with miners in distress. FRITSCH had to be very careful to avoid disturbing influences from rail installations, pressure conduits or electrical cables which, by guiding electromagnetic waves, give rise to unfoundedly large propagation distances. The reception of the Innsbruck radio transmitter (570 kc) was also significantly better in mine workings with rail installations than in such as had no metallic connection with the surface.

For our preliminary experiments we constructed a small battery powered vacuum tube transmitter which radiated at a power of almost 1 watt at a frequency of 200 kc. A 20 cm long ferrite rod was chosen as a transmitting antenna which simultaneously carried the PA-circuit of the transmitter (Fig. 2,1 Fig. I).

A commercial portable radio receiver (Radione R22T) was used as a transistor receiver, after having been modified

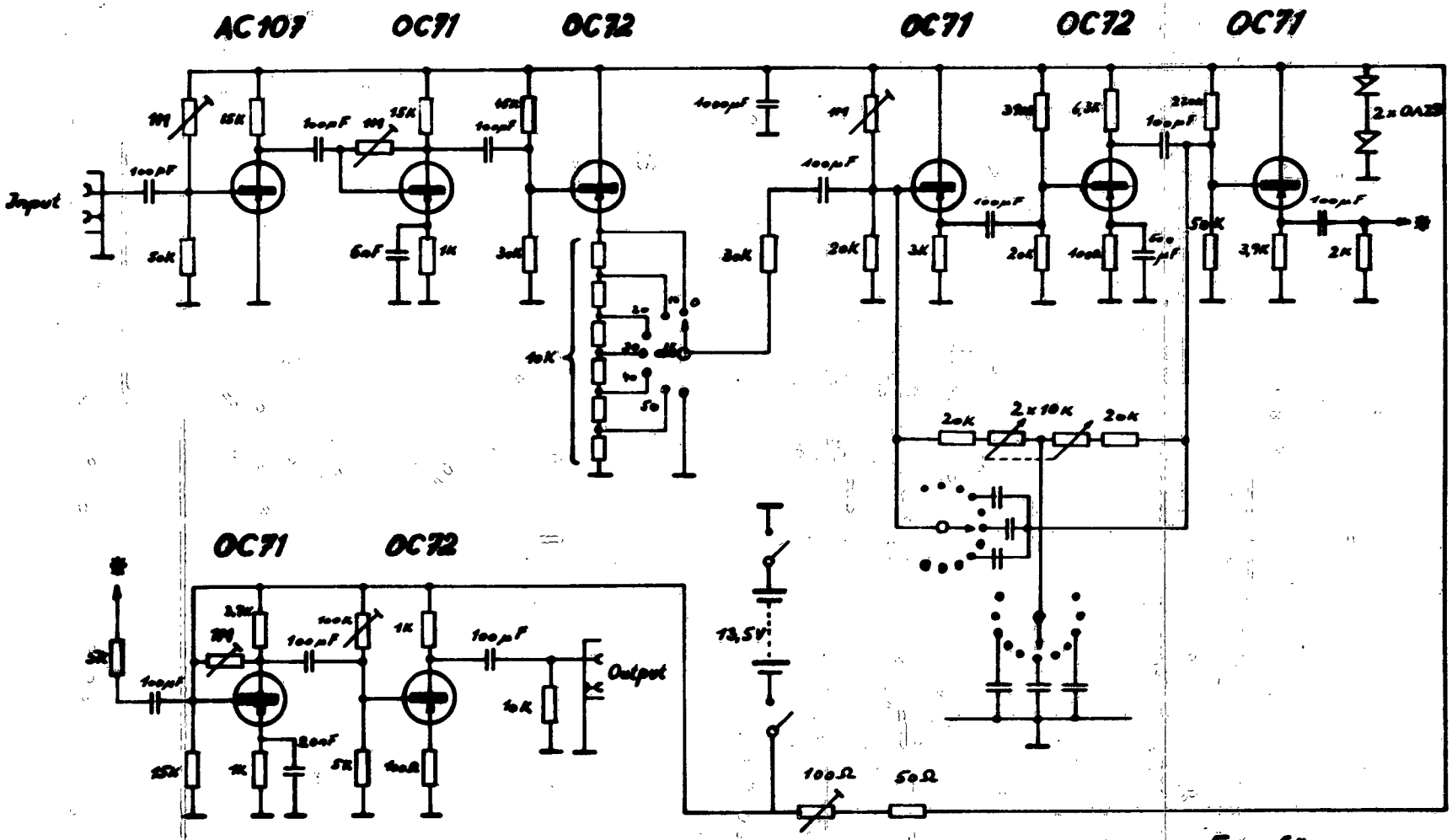
AC107
OC71
OC72
OC71
OC72
OC71
Input
OC71
OC72
Output
12,5V
100Ω
50Ω
Empfänger
Receiver

Fig. 2,6

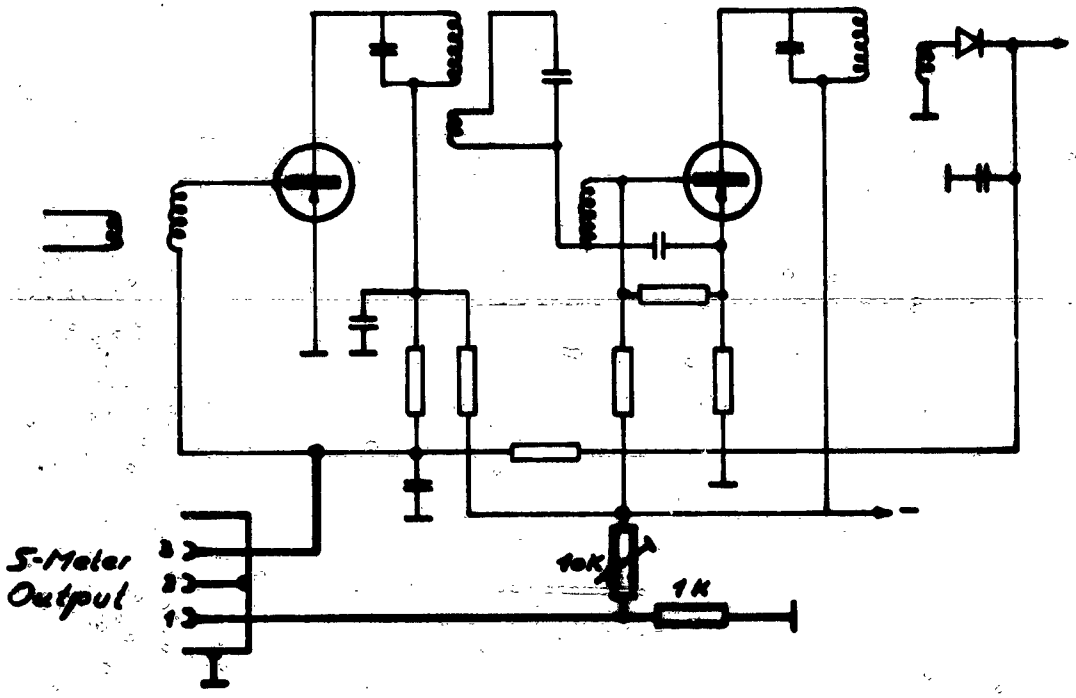

Radione R22T Fig. 2,2

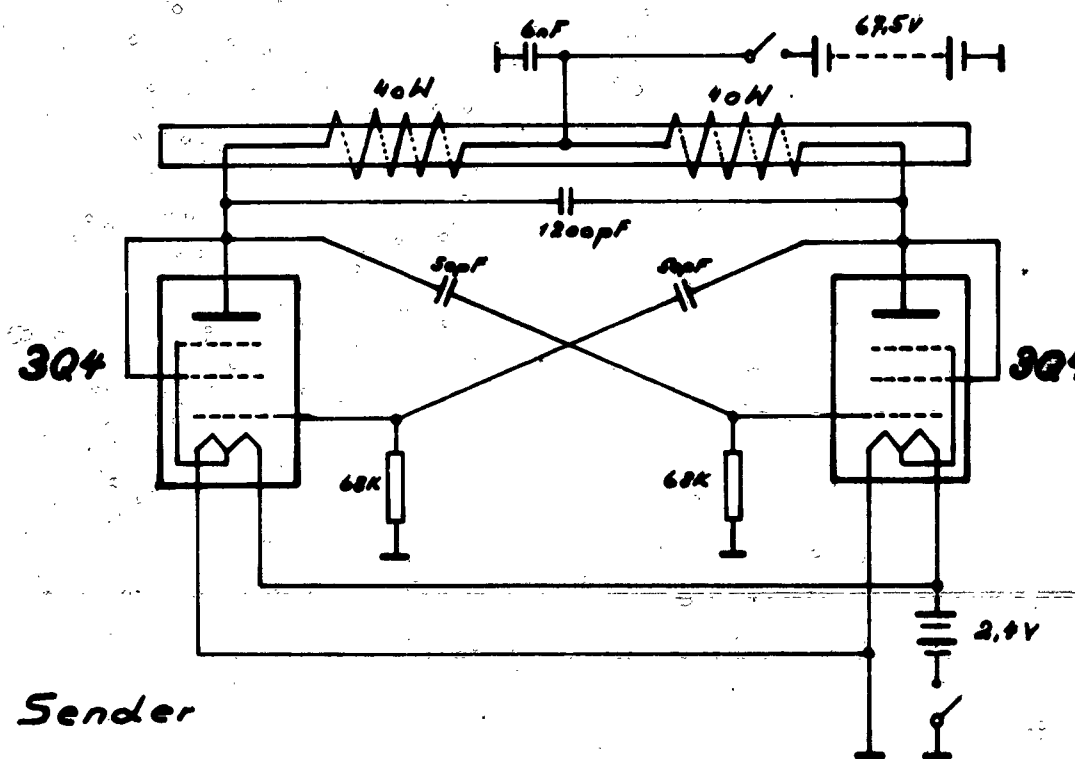

Sender

Transmitter Fig. 2,1

for this special purpose (Fig. 2,2). The control voltage has been lead out to terminals where it is measured by means of a transistor d.c. voltmeter (S-meter) (Fig. 2,3). Although the receiving unit (Fig. V) had not been calibrated in field strength units, it was nevertheless possible to estimate the reception results in a qualitative and quantitative manner. The attained propagation distances were moderate owing to the small transmitter power available.

The purpose of these experiments was to obtain a general survey of the directional characteristics of ferrite antennas. Several informative measurements were carried out above ground on level terrain as well as in underground locations. The decrease of field strength as depending on the distance and the directional characteristics was measured both with horizontal and vertical antenna position. A dependence upon the degree of soil moisture could also be established. As for the remainder the same results were found which are discussed below in the section on the transmitting antenna SAIII.
Apart from this, initial measurements of the field strength of the Innsbruck radio transmitter were also carried out. The field could be ascertained to large depths in the main gallery.

2,2 E q u i p m e n t S e c t i o n

<u>VLF Measuring equipment</u>

Transmitter:

The transmitter that has hitherto been used for the measurements consisted of the following parts: batteries,

RC-generators, transmitter amplifier, exchangeable transmitting antenna, support for the antenna.

The individual sections were connected after arrival at the site by means of leads. Thus the transmitter was prepared for operation (Fig. II).

A transistor, type Levell TG150M RC-generator was used as oscillator, supplying a maximum output voltage of 2.5 V, which could be attenuated by steps of 20db each. It operated in a frequency range from 1.5 c to 150 kc. The a.c. voltage supplied by this generator was used to drive directly the

Transmitter amplifier:

This amplifier has been developed in our laboratory and is designed as a 20 watt low frequency amplifier; it is mounted with TF78, 3 x TF80/30 transistors (Fig. 2,4). Power is supplied from two lead accumulators 6V/7Ah. The amplifier draws 3.5 A at full operation, which is equivalent to an efficiency of 50%. The capacity of the batteries allows a two-hour operation.

The transmitter amplifier has been designed such as to permit the connection to a symmetrical or an unsymmetrical load. The power transformer is cut in or out as required by the mode of operation.

The maximum power of 20 watts supplied by the transmitter has been used to generate a powerful magnetic field which is radiated by the antennas.

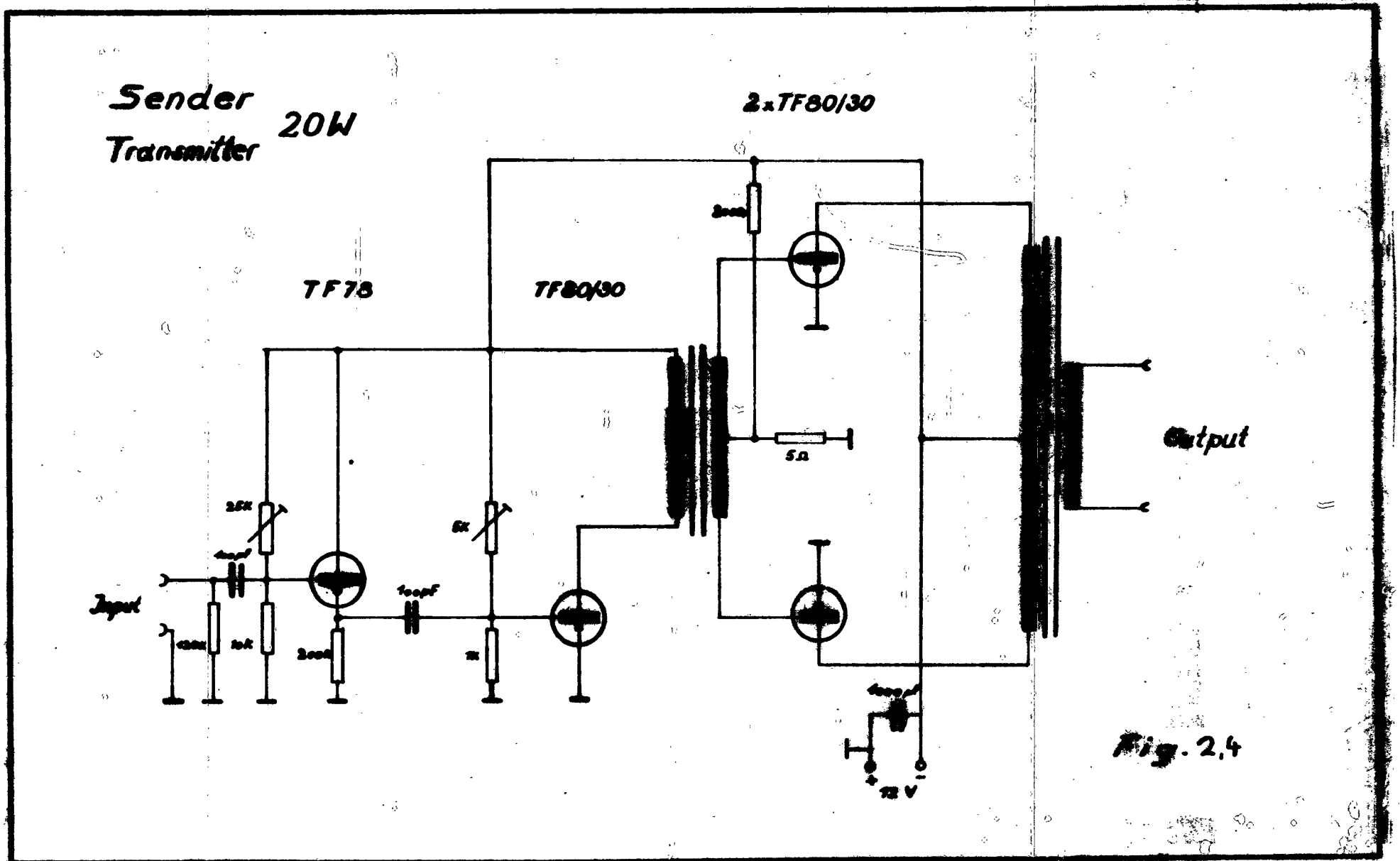
Sender
Transmitter
20W
2xTF80/30
TF78
TF80/30
Input
Output
5Ω
12 V

Fig. 2,4

Transmitting antennas:
To date, four different types of antenna have been built (SAI to SAIV). Initially a procedure was chosen by which a coil with a very high inductance was wound on an iron core. In order to eliminate the disturbing influence of the reactance of the coil, the inductivity L was parallel-connected to a capacity C to constitute a parallel resonant circuit which was tuned to the operating frequency. This measure simultaneously brought two more advantages: first, the power transformer and the losses generated therein could be eliminated by a symmetrical design of the antenna, because it was fed through two taps located symmetrically about the center (in which instance care had to be taken to obtain the correct impedance). Secondly, the current through the coil was increased as in every resonant circuit (Fig. 2,5).

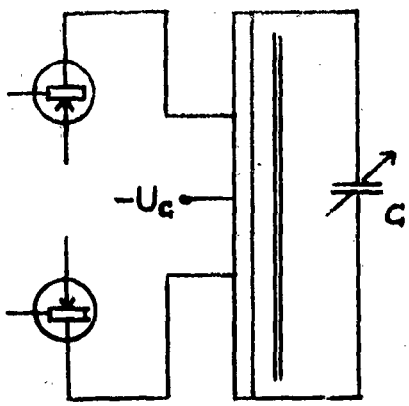

Fig. 2,5

For every parallel resonant circuit there holds the relation that the partial currents J_L and J_C are larger by the ratio expressed by Q, the figure of merit of the circuit, than the total current J passing through the circuit.

The phase shift of 90° between J_L and J_C occurring at resonance has no disturbing influence, because the stationary magnetic field does not store energy, so that it can as well be generated by a reactive current. The energy required to cover the radiation and eddy current losses in the rock can be regarded as being negligibly small.

On the basis of these considerations it was possible to design the antenna in such a way as to utilize the total energy supplied by the transmitter to compensate for the ohmic losses in the antenna only.

Design data of the transmitting antennas SAI and SAII (Fig. III).

Transmitting antenna I:

Iron rod length: 100 cm, sheet material IV
Iron cross section: 6 cm^2
Turns number: 2 x 96 turns, conductor: 2 mm diam. copper
Ohmic resistance: 185 mΩ
Inductivity: 3.2 mH
Taps at ± 25 turns, symmetrical about the center

Transmitting antenna II:

Iron rod length: 100 cm
Iron cross section: 3.5 cm^2
Turns number: 2 x 450 turns, conductor: 0.75 mm diam. copper
Ohmic resistance: 3.1 ohms
Inductivity: 80 mH
Taps at ± 25 turns, symmetrical about the center

It appeared, however, that in practical operation these antenna forms did not perform satisfactorily, because the

effective surface was too small and the losses in the iron core were too large. For this reason, henceforth other measures were adopted in the development of the transmitting antenna SAIII. The iron core was removed; in order to compensate for the resulting loss in inductivity, the diameter of the coil was increased to such an extent as to keep within the dimensions of the mine workings. This method afforded the following remarkable advantage:

The magnetic field in the axis of an air-core coil which may be regarded as an n-fold circular loop, can be calculated in the vicinity of the transmitting coil from the following formula:

$$B \left[\frac{Wb}{m^2}\right] = \frac{J_o n_o R^2}{o 2(R^2 + r^2)^{3/2}} \quad [A.m]$$

The turns number was chosen as large as was permitted by the ohmic resistance determining the figure of merit of the circuit and the resonant resistance. Another, in no way less significant limit for the turns number was the copper weight, because in consideration of the required low resistance and the maximum permissible current the cross section could not be chosen too small. It is worth noting that the copper weight of SAIV is more than 17 kg and that the complete antenna, weighing 20 kg, cannot easily be transported in narrow mines. As has been shown by theoretical investigations it is more convenient to wind a coil from very few turns, but with a diameter as large as possible for a given wire length in order to obtain a maximum magnetic moment.

The transmitting antennas SAIII and SAIV were built according to these considerations. The majority of measurements

was carried out with the SAIII.

If an iron core is absent, it is possible to determine the experimental conditions uniquely by stating the frequency and the current J through the transmitting coil. The reactance of the coil was, as before, made to vanish by means of a series connection with a condenser of a capacity suitable for the frequency used in the experiments. The resonant resistance R_o is identical to the ohmic resistance of the coil and kan be kept within small limits by increasing the conductor cross section in order to obtain large currents J. If the transmitter power N and the resonant resistance R_o is given, the current is calculated from $J = \sqrt{N/R_o}$.

In order to match this transmitting antenna to the amplifier output a power transformer of suitable dimensions is required. The current in the antenna circuit is being measured with a Philips instrument of the type P 81700/01. In order to prevent a reduction of the figure of merit of this circuit by a too low LC ratio at the given low frequencies it was necessary to increase the inductivity of the transmitting coil.

For the coil designs used L is calculated from

$$L\ [\mu H] = n^2 2\pi\, D\left(\ln \frac{4D}{\sqrt{b^2 + c^2}} - k\right).10^{-3} \qquad [cm]$$

where k = form factor, depending on c/b
k ~ 0.48 for SAIII
n = turns number

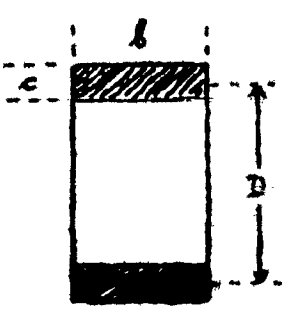

Design data of the antenna SAIII (Fig. II).

Diameter D = 98 cm
Winding width b = 2 cm
Winding height c = 1 cm
Conductor cross section: 1.2 mm diam. copper
Inductivity: 5 mH
Ohmic resistance: 1.1 ohms

To date, the investigations have been limited to dipole antennas. The question, whether antenna forms of higher order, as quadripoles, for instance, will provide better results, must be decided by further theoretical studies.

All antennas of a dipole character possess a directional characteristic depending on the angle φ. It appeared from the measurements that in the direction of the dipole axis the field strength is twice that perpendicular to it. This φ-dependence has been established by separate measurements. As regards the measuring technique, difficulties were encountered in adjusting the transmitting antenna in the mine in such a way as to ensure coincidence of its axis with the straight line connecting transmitter and receiver. When mine maps were available this direction could be found by means of a compass. If this was not the case it had to be found empirically. It can be seen from the antenna characteristic, however, that an error in the directional adjustment of $\pm 20^{\circ}$ causes an error in the field strength of no more than 5%.

The receiver amplifier:
For detecting the magnetic field radiated by the transmitting antenna an 8-stage selective amplifier equipped with transistors 1/AC107, 4/OC71, and 3/OC72 was used.

The circuit schematic is shown in Fig. 2,6.

The input voltage which had to be expected is of the order of μV. The first large-gain amplifying stage had therefore to be designed with a particularly low noise level.

The input stage is succeeded by two more amplifying stages, the second of which serves as an impedance matcher. Owing to the low output impedance of this stage it was possible to use an attenuator with a low ohmic resistance in the next stage. The calibrated potentiometer being used for it permits to attenuate the input voltage by 10 db steps down to 50 db. Hence it is impossible to overdrive the subsequent stages.

Following the calibration potentiometer is a selective amplifier consisting of a two stage transistor amplifier which is mutually coupled by a bridged T-section. The coarse adjustment of the chosen frequency is effected by staggering the condensers of the network in 11 steps, thereby varying the frequency from 20 c to 50 kc; the fine adjustment is accomplished by setting the resistances for which double potentiometers have been used.

The following stages of the amplifier step up the signal until it attains an output value of several volts.

The use of a selective network afforded a substantial increase of the input sensitivity because, as is generally known, the noise voltage varies inversely as the band width. It is, however, also desirable to have the amplifier possess only a low susceptibility to external disturbances or stray fields which feature should go with a

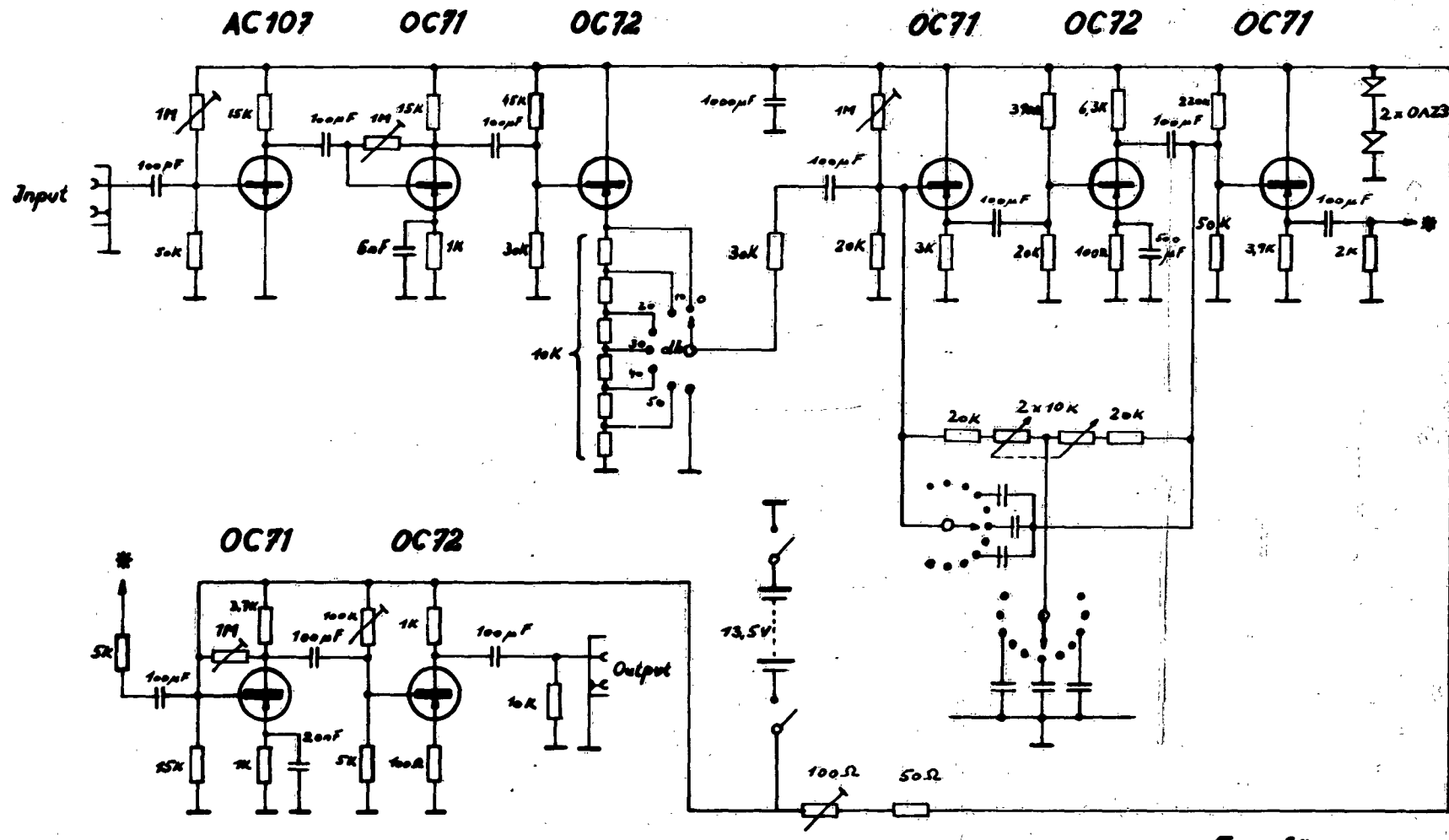

Fig. 2,6

Empfänger
Receiver

Fig. 2,7

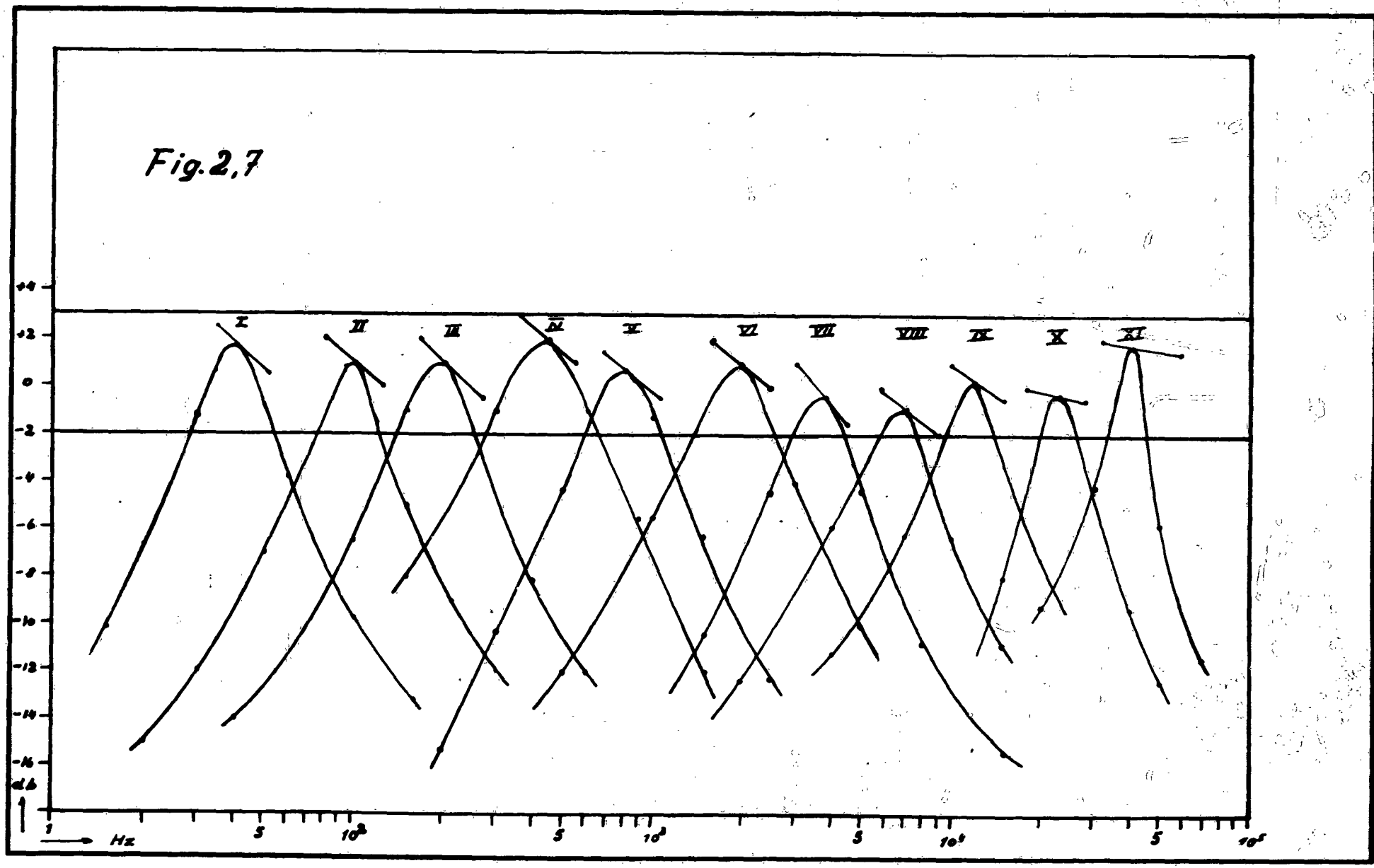
I
II
III
IV
V
VI
VII
VIII
IX
X
XI
+4
+2
0
-2
-4
-6
-8
-10
-12
-14
-16
dB
1
Hz
5
10²
5
10³
5
10⁴
5
10⁵

reduction of the noise level. A new receiver model is now being constructed in which it is aimed to attain an enhancement of selectivity and, at the same time, an increase in sensitivity.

Design data of the receiver amplifier

Input sensitivity: 2 μV
Signal-to-noise ratio: 30 db
Gain: 113 $\pm$ 3 db in the entire frequency range, adjustable in steps of 10 db each
Operating voltage: 3 x 4.5 V flashlight batteries stabilized by two Zener diodes.
Input impedance: 10 kΩ
Output impedance: 800 Ω
Frequency range: 20 c - 50 kc, subdivided into 11 ranges.
Band width: 0.4 (at 10 kc)

An internal view of the amplifier is shown in Fig. VI.

The overall gain of the amplifier is in the region of $4.5 - 4.7\ 10^5$. Originally it depended markedly on the level of the supply voltage which was taken from three series-connected flashlight batteries. This disturbing effect was eliminated by stabilizing the operating voltage of the first six stages by means of two Zener diodes OAZ3. The residual fluctuations are now less than $\pm$ 0.2 V. The output voltage is constant to within 3 db over the entire range, as can be seen from the frequency characteristic. The residual error is eliminated by a control procedure which consists in checking on the amplification in the laboratory every time one series of measurements in the mines had been completed. This was done at exactly the same frequencies as were used in the field.

The output signal of the receiver amplifier is fed into the oscilloscope Tectronics type 321 for measurement. This affords a measurement of the amplitude of the signal and of its frequency together with an estimate of eventual disturbances.

Initially the oscilloscope could not be used for these measurements, because the receiving antenna which had been placed at a distance of only two meters from the oscilloscope picked up the entire stray field from it. High voltage in the oscilloscope is produced by two blocking oscillators operating at frequencies of 2 kc and 20 kc which radiate a powerful frequency mixture rich in harmonics. Hence it was required to place the oscilloscope into a casing of 1 mm sheet iron, to shield the battery leads very carefully and to filter the battery voltage after entering the casing. In order to ensure longer operation of the oscilloscope, power was taken from two separate 6 V accumulators which had also to be placed in a casing.

For some measurements, especially at small ranges or in difficult locations a transistor millivoltmeter (Levell TM2B) was used to replace the oscilloscope. In Fig. IV the complete receiving equipment is shown.

The receiving antennas

Great difficulties were encountered in the construction of the receiving equipment when it came to the design and the construction of the receiving antennas (termed EA....). As has been shown in the theoretical section the design must aim at balancing in the most favorable

These factors are: inductivity, effective cross section, spurious winding capacitances and the ohmic resistance of the conductor wire. A large inductivity can either be achieved through a ferrous-cored coil with only a few turns, or by an air-core solenoid with many turns and a large diameter (cross section). The problem that had to be solved now was to find the most efficient design by means of theoretical evaluations and practical experiments.

Design data of the receiving antenna EAI: it consisted of a ferrite rod on which two series-connected crossed coils with a very high inductivity were wound.

Technical data of the antenna EAI:

Length of the ferrite rod: L = 47.5 cm
Diameter/cross section: d/F = 1.5 cm/1.77 cm^2
Ohmic resistance: 135 ohms
Inductivity: L = 0.8 H (= 1000)
Receiver inserted at the mid-point of the winding.
(See Fig. 2,8 just below).

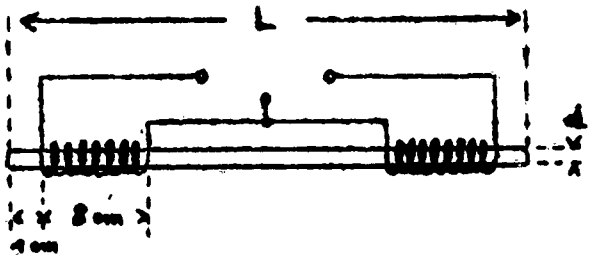

Fig. 2,8

In Fig. VII is shown the antenna with the static shield removed.

The antenna was connected to a variable capacitor to form a parallel resonant circuit. Thus it could be adjusted to the frequency of the transmitted signal.

The winding is tapped at the center, where the receiver input is connected. The figure of merit of the resonant circuit is relatively high, owing to the large RC-ratio and the low capacity of the winding. The voltage gain resulting from this is given by the factor Q = 10. Owing to the small geometrical dimensions the antenna can easily be shielded against electric fields by means of an aluminum foil. Hence it is only little susceptible to disturbing fields, thus permitting the utilization of the full sensitivity of the amplifier.

An increase of the sensitivity, the figure of merit remaining constant at the same time, can be achieved by an increase in the cross section of the iron core. Another method would consist in placing several antennas of the EAI type side by side and to series-connect them. Studies in this direction are being made.

The receiving antennas EAII and EAIII were built according to a principle differing from that of the ferrite antenna.

The antenna EAII consisted of a slender toroidal solenoid. Its electrical performance data were very unfavorable so that it was not used for further measurements.

Improvements were achieved in the design of the antenna EAIII. It consists of a cylindrical coil with 1000 turns, having a diameter of 45 cm. It was shown by underground measurements that the sensitivity of this antenna is better than that of EAI by a factor of 2 - 2.5 (at 10 kc), but that the directional sensitivity is worse. In spite of this fact this type of antenna has proved to constitute the most favorable design. The receiver is connected

to a tap, the position of which is determined emperically. Similar to the EAI this antenna is also tunable to resonance by means of a variable capacitor and a step-type group of fixed capacitors.

Fig. IV shows the receiving unit and conveys an impression of the size and appearance of the EAIII antenna.

2,3 Underground Measurements

Calibration of the receiver unit

The receiver equipment consists of several portable units; it comprises the interchangeable receiving antennas which are tunable to the transmitted frequency, the calibrated selective amplifier and a battery powered oscilloscope. To this is added the portable, metal sheathed kit for three 6V/4.5Ah accumulators which serve as a power supply for the oscilloscope, because built-in batteries would permit operation for no more than about one hour. The receiving antennas are interchangeable; hence it can easily be arranged that different antenna types are used during one underground measurement, either to find the best position of the antenna or to limit the experimental error by means of repeating the measurements with different antennas.

The receiving unit was considered to perform satisfactorily when it permitted the determination of the magnetic field strength from the oltage measurements at the amplifier output. The field strengths in our experiments were of the order 10^{-12} [Wb/m^2]. From this value can easily be inferred that for calibration operations

a location had to be found where disturbing magnetic fields could be kept to a minimum. AA detailed study of commercially available Faraday cages has shown that none of them meets the rigorous requirements as concerns magnetic shielding against low-frequency fields. From these considerations it appeared most convenient to conduct the necessary calibration measurements underground where conditions are naturally the same as for the actual measurements.

The calibration consisted in generating a magnetic field of known magnitude, inserting the receiving antenna into this field and measuring the output voltage of the receiver. The values of the measured voltage thus obtained were then converted back to the input voltage; this voltage was plotted against the known field strengths. The transmitting antenna was directly used for the generation of the calibration magnetic field. According to the formula

$$B = \mu_0 \, n \, J \, R^2/2(R^2 + r^2)^{3/2}$$

the desired field strength which was measured at a distance of about 10 m from the transmitting antenna could easily be adjusted by a variation of the current J. Some difficulties were created, however, by the necessity to eliminate undesired effects, as, for instance, the influence of stray electrostatic fields.

Calibration of the receiving antennas EAI and EAIII (Fig. 2,9)
Frequency 10 kc, r = 12 m, transmitting antenna SAIII.
Parametric variation of J (mA).

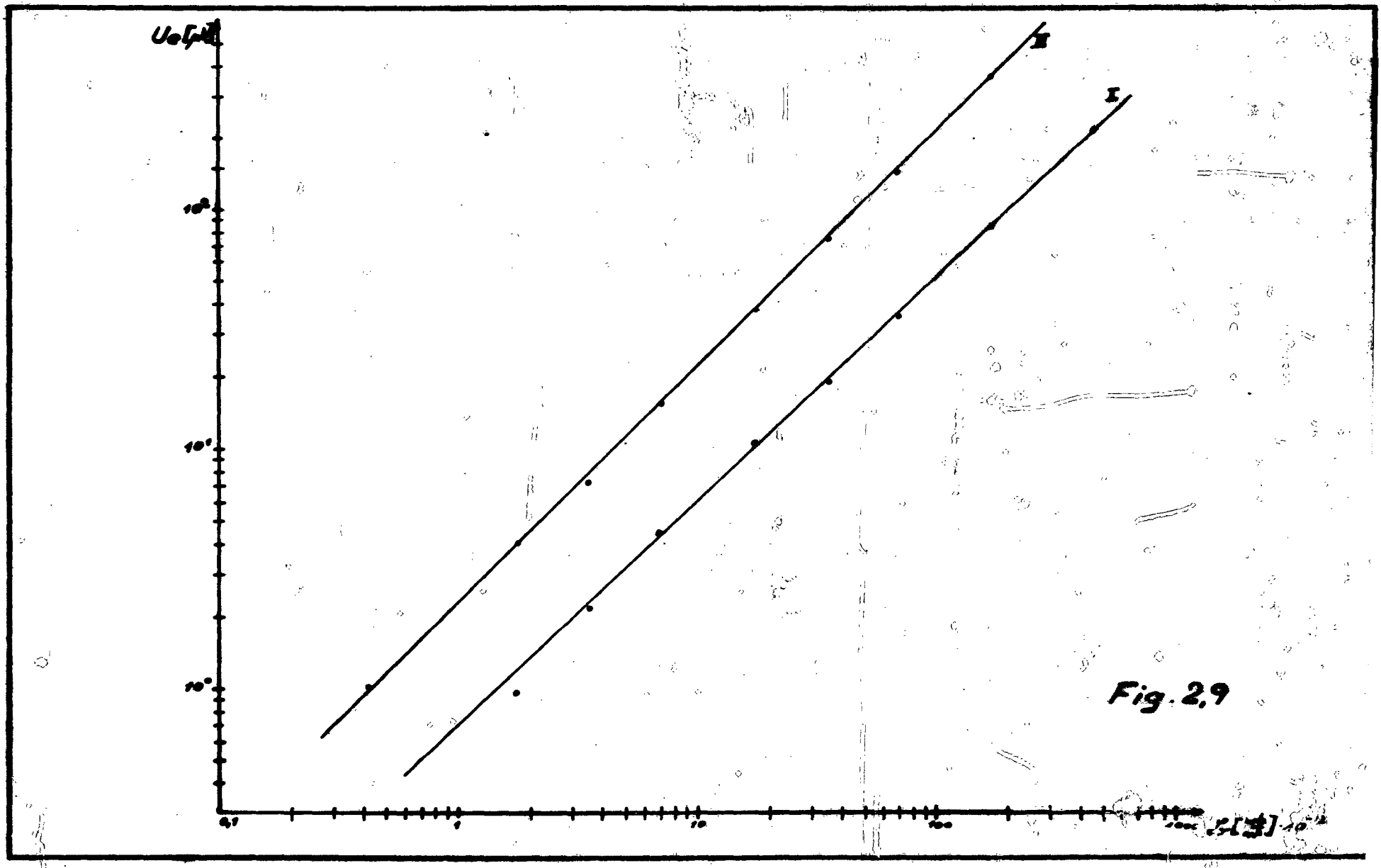

Fig. 2.9

EAI J [mA]	U_e [μV]	B [$\frac{Wb}{m^2}$].10^{-12}	EAIII J [mA]	U_e [μV]	B [$\frac{Wb}{m^2}$].10^{-12}
49	88.6	171.5	48	360	168
20	36	70	20	145.5	70
10	19.2	35	10	76	35
5	10.6	17.5	5	38	17.5
2	4.5	7	2	15.6	7
1	2.15	3.5	1	7.2	3.5
0.51	0.95	1.78	0.51	4.05	1.78
48	88	168	0.23	(1.27	0.805)
			0.12	1.01	0.42
			51	380	178

$$B = \mu_0 \frac{n.J.R^2}{2(R^2 + r^2)^{3/2}} = 3.5.10^{-12}.J \quad (mA)$$

Propagation measurements

After the calibration had been successfully completed, the quantitative propagation measurements of electromagnetic waves in rock could be started.

Interest in these measurements was centered about a check on the predictions offered by theoretical considerations concerning the decrease of field strength over distance in rock with a varying degree of conductivity. The test frequency was initially settled at 10 kc. This choice was justified by the imitations inherent to the transistor amplifier , because, owing to efficiency considerations, the available power transistors did not permit the use of higher frequencies. On the other hand, the design of the transmitting antenna imposes a lower limit on the measuring frequency which is about 2 kc. It will be the aim of further investi-

gations to reach lower values by a systematic reduction of the frequency.

In the sequel we will select from the numerous field strength measurements that have been made in three different mines, four representative experiments, and offer a detailed discussion of them.

The field locations were selected on the basis of mine maps and inspection tours. They were considered particularly favorable, if electrical or fluid conduits or rails were absent in the workings. Secondly it was desirable to have no large cavities in the immediate neighborhood of the transmitter and in particular not near the straight line connecting transmitter and receiver; still the system should be of sufficient extension as to permit measurements at intervals of about 20 m. Care was also taken to obtain at least an approximate picture of the geological structure of the rock along the workings connecting the measurement locations. Fortunately no great difficulties arose in finding such locations in the mines inspected for that purpose.

After the transmitter had been transported to the selected location and the orientation of the antenna had been completed with the help of mine maps and a compass, the receiver was carried to the individual measuring locations; the antenna used in one particular experiment was adjusted to give maximum field strength. Subsequent to this the voltage occurring at the amplifier output was measured. Depending on variations in the ambient conditions in the rock, distances reaching to 220 m could be bridged.

Curves 1 through 4 in Fig. 2,10 illustrate the results of the experiments. It can easily be discerned that the individual series of measurements in the diagrams deviate strongly from one another. This may be explained by variations in the parameters ϵ and $\varkappa$. $\varkappa$ was determined, as has been explained in the theoretical section (1,1), from tables and through measurements, and further digression on this problem does not fall within the scope of this section. Further considerations will be consecrated to a discussion of the influence of the conductivity parameter only.

Measurements in the St. Gertraudi mine (Großkogel), mine map no. 1.

The transmitter was placed in locations EVII and EIX, the measuring frequency was 10 kc, the antenna current 1.25 A, the antenna used was SAIII.

Results:

Measuring location	dist. m	U_{eI}	U_{eIII}	$\|B\|_I$	$\|B\|_{III}$	$\|B\|^*$
-	/ 20	-	-	-	-	1
1	/ 23	300	500	650	240	0.77
2	/ 38	95	150	185	70	0.23
3	/ 56	32	60	60	28	0.09
4	/ 75	18	30	32	14	0.045
5	/ 95	9.9	18	17	8.2	0.026
6	/ 115	5.6	8.5	9.3	3.8	0.012
8	/ 137	-	5.6	-	2.5	0.0081
9	/ 185	-	1.9	-	0.85	0.0027
10	/ 125	-	0.8	-	0.35	0.0011

The values given for the modulus of the magnetic field strength are plotted in Fig. 2,10. Every series of values has subsequently been converted to the extrapolated field strength at 20 m distance in order to afford a satisfactory comparison of the curves. Two theoretical curves have been added which have been calculated for a conductivity $\varkappa$ of 10^{-3} and 10^{-4} [$ohm^{-1}m^{-1}$]. Without exception, the experimental curves keep within the limits drawn by the theoretical curves.

A behavior similar to that of curve no. 1 is shown by the series of measurements recorded in the Schwaz mine. The conductivity there is of the same order and the rock in the two locations is also of the same nature.

Measurements in the Schwaz mine; mine map no. 2.

The transmitter was placed in location no. 4; the measuring frequency was 10 kc, the antenna current 1.25 A, the antenna used was SAIII

Results:

Measuring location	dist. m	U_{eI}	U_{eIII}	$\|B\|_I$	$\|B\|_{III}$	$\|B\|^*$
-	/ 20	-	-	-		1
-	/ 25	128	520	225	250	0.63
0	/ 47	30	120	55	56	0.14
a	/ 60	16	60	28	28	0.07
b	/ 78	85	30	14.5	14	0.035
c	/ 98	4.5	15.6	7.2	7.2	0.018
d	/ 115	2.8	9	4.4	4.1	0.0105
e	/ 133	1.9	5.6	2.9	2.6	0.0068
f	/ 150	1.27	3.15	1.5	1.1	0.0032
g	/ 186	0.76	1.9	1.1	0.85	0.0025
h	/ 196		1.27		0.5	0.0012

The measurements are plotted in curve no. 2 (Fig. 2,10).

Results differing substantially from these have been obtained from the experiments in the

Lafatsch mine, mine maps nos. 3a and 3b.

The rock in the vicinity of this field location is interspersed with lead-zinc ores. The increase of conductivity resulting from this circumstance is markedly expressed in the curves nos. 3 and 4 (Fig. 2,10). The striking flattening-out of the third experimental curve can possibly be traced back to a disturbance in the measurement. It may be explained by the fact that the measuring locations (e) to (i) are connected by rail installations. This may be the reason for a falsification in the decrease of field strength over distance function. More favorable workings were available for the second measurement in the same mine. The distance was chosen somewhat shorter, it traversed, however, rock even more interspersed with ore. The influence of the ore content is plainly discernible, because the conductivity is three to four times that in the Schwaz mine. It is worth noting that this conductivity is averaged over the entire volume, thus differing from that determined from rock samples.

Measurements in the Lafatsch mine, (series no. I).

The transmitter was placed in location II, the measuring frequency was 10 kc, the antenna current 1.25 A, the antenna used was SAIII.

Results:

Measuring location	dist. m	U_{eI}	U_{eIII}	$\|B\|_I$	$\|B\|_{III}$	$\|B\|$ *
- /	20	-	-	-	-	1
α /	31	125	600	250	280	0.37
β /	52	31.8	127	57	57	0.082
γ /	80	9.2	38	15.5	17.5	0.023
δ /	105	3.6	16.3	5.7	7.5	0.0086
ε /	130	1.8	7.9	2.8	3.6	0.0043
ζ /	161	1.1	3.8	1.6	1.7	0.0023
ι /	226	0.3	2.2	0.4	1	0.00086

Measurements in the Lafatsch mine, (series no. II).

The transmitter was placed in location II, the measuring frequency was 10 kc, the antenna current 1,25 A, the antenna used was SAIII.

Results:

Measuring location	dist. m	U_{eI}	U_{eIII}	$\|B\|_I$	$\|B_{IIII}$	$\|B\|$ *
α' /	20	620	2000	1400	1000	1
β' /	43	28.5	220	60	100	0.1
δ' /	71	8.3	28.5	14	13.5	0.014
ε' /	81	5.6	18.4	9.2	8.5	0.0093
η' /	103	2.5	7.9	3.9	3.6	0.0037

In column no. 1 the receiver positions are enumerated and their distance from the transmitter is given. Columns nos. 2 and 3 contain the voltages measured when the receiving antennas SAI and SAIII were used; they are given in μ V, converted back to the amplifier input. By means of the diagram in Fig. 2,9 it is possible to derive the

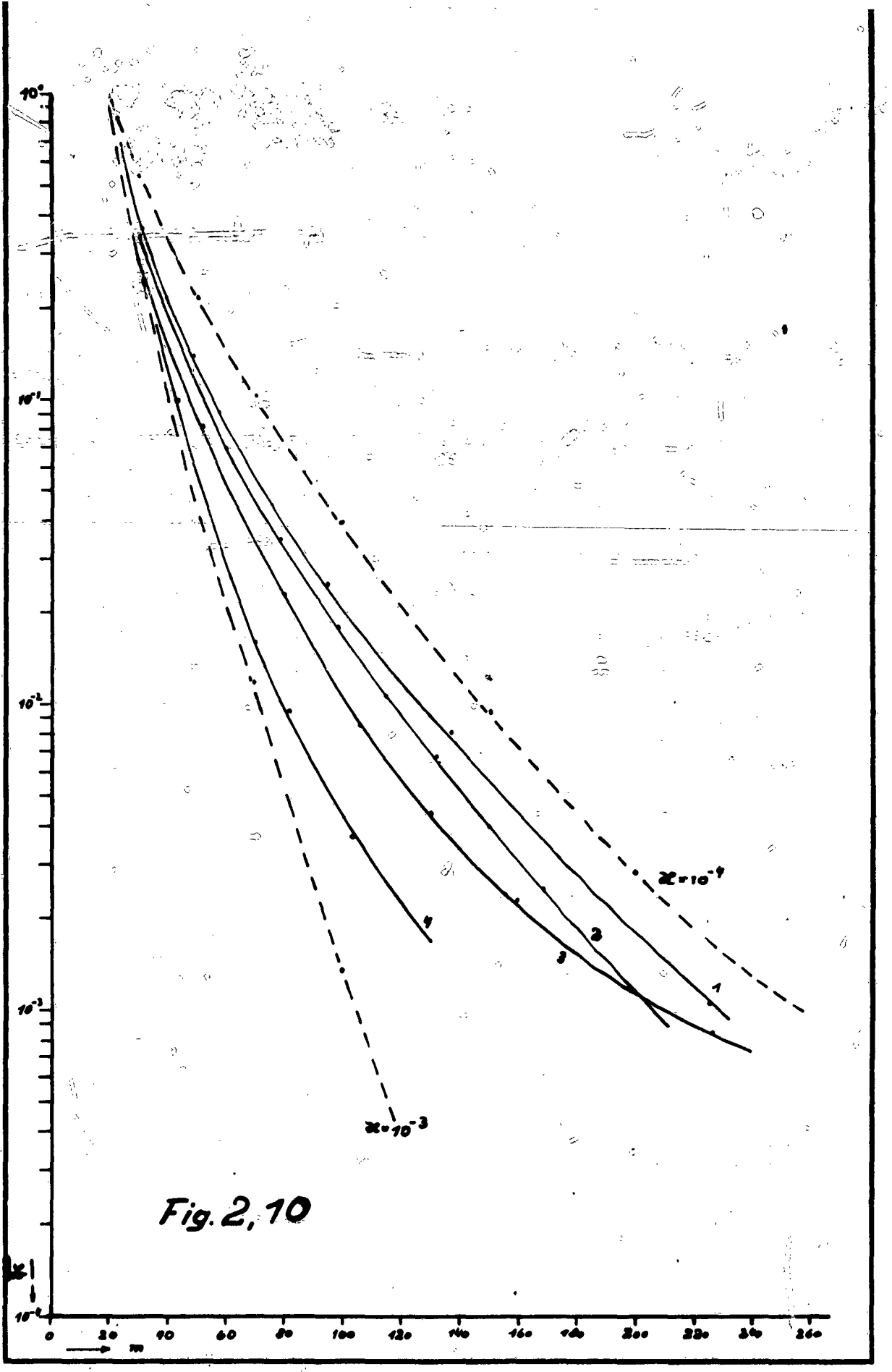
10^0
10^{-1}
10^{-2}
10^{-3}
10^{-4}
0
20
40
60
80
100
120
140
160
180
200
220
240
m
$\alpha = 10^{-4}$
$\alpha = 10^{-3}$
1
2
3
4

Fig. 2,10

field strength values from these voltage levels given in column 4 and 5. In the last column the values averaged from column 4 and 5 are given, extrapolated to the field strength at 20 m distance. This field strength has been assumed as unity.

Special Measurements

The work described to this point has absorbed the major portion of the available time. However, efforts were also made to study problems connected with the measuring apparatus. Of special interest was an exact determination of the antenna characteristic which bore special weight in the theoretical work.

These measurements were conducted as follows: the transmitter was placed in a large underground cavity in the Schwaz mine ("Messerschmitthalle"); the field strength was then measured at a distance of 12 m in order to establish its dependence on the angle φ. The results are illustrated in Fig. 2,11. It can be clearly seen that the field strength in the direction of the axis of the transmitting antenna is twice as large at a certain distance than in a direction perpendicular to the antenna axis at the same distance.

Results:

angle (°)	|B|	orientation of B (°)
0	1	0
45	0.78	65
90	0.5	0
135	0.78	65
180	1	0
225	0.78	60
270	0.5	0
315	0.78	85
360	1	0

Fig. 2,11

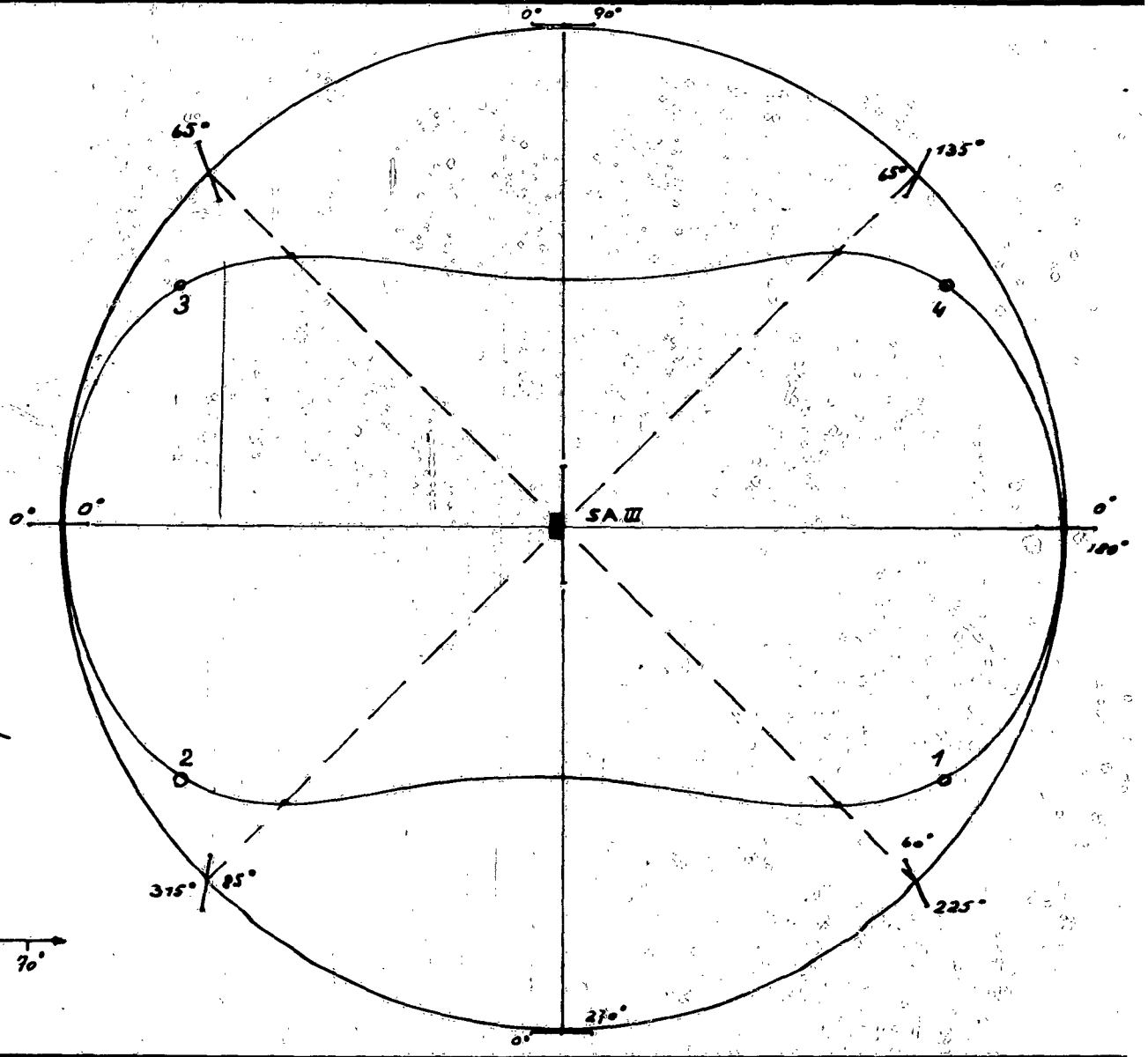

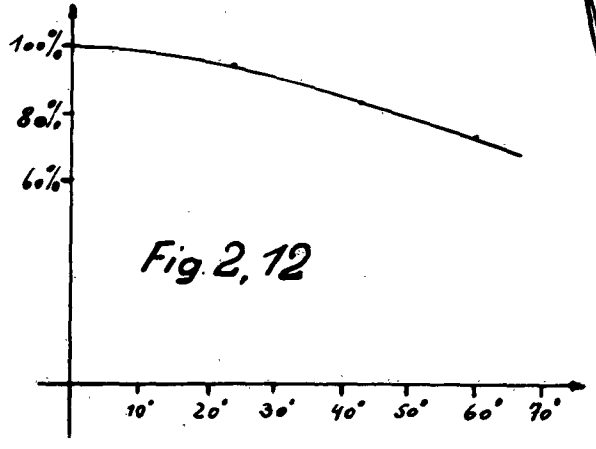

Fig. 2,12

After these measurements had been completed the error arising from incorrect adjustment of the antenna was closely investigated, using the Schwaz mine (mine map no. 2) as field location. In order to obtain practically useful values, a distance of about 50 m between transmitter and receiver was chosen. The transmitter, being placed in location no. 4, was initially oriented towards the first measuring location no. 0. The receiver was then moved to other locations (a',b',c'). The field strength versus φ function as derived from these measurements is plotted in Fig. 2,12 through an angle of 60°. The results have already been anticipated in the section on transmitting antennas (2,2). For a misorientation of about 20° the error does not exceed 5%.

Concluding, some remarks are appropriate concerning experiments of a special nature, referring to the measuring locations in the mine maps nos. 1 and 2, which have not been discussed as yet.

The first VLF measurements were conducted in the St. Gertraudi mine, a frequency of 30 kc being used for the experiments. The distances that could be bridged were relatively small owing to the unfavorable antenna design (SAI and SAII), the comparatively high frequency used, and the low transmitter power (transmitter location SVIII, receiver location EVIII). Further measurements which cannot be discussed in detail in this report were carried out in the Schwaz mine. Their purpose was to establish the influence of a body of gray copper ore extending between the locations nos. 1 and 2 parallel to the main working (1 - 4).

As a calibration facility an orefree distance of 160 m length was chosen between the locations 5 and 6. At a measuring frequency of 10 kc the field strength dropped to 3% of the original value. Maintaining the same experimental conditions the field strength was then measured between locations 1 and 2, the transmitter being placed in 1 and the receiver in 2. Along this traverse the field strength decreased to no more than 2%. This remarkable divergence has been traced back to the influence of a closed iron loop consisting of tubing in the working no. 2 and of rail installations in the workings 1 and 8; it was not due to the action of the orebody. Depending on the orientation of the transmitting antenna, either parallel or perpendicular to the rails, the field strength in location no. 2 was large or small. These phenomena are still being investigated more closely.

Recently attempts were made to bridge larger distances (to 300 m) using the same transmitter and a transmitting frequency of 5 kc. Between locations 4 and 2, or 7 respectively, definite field strength measurements could be made. The results of these experiments will be presented in a later report. It was substantiated beyond doubt that the theoretical considerations predicting a less pronounced attenuation of low frequency electromagnetic waves in conductive media are correct.

3. Geological-mineralogical Section

3, 1 General Geological Survey

It has been explained already in Sec. 2,3 that the experimental investigations were carried out in mines in the Tyrol. The Schwaz mine, 26 km by road east of Innsbruck and the St. Gertraudi mine, 44 km by road east of Innsbruck, are both situated on the northern slope of the "Tuxer Gebirge" (Tux mountains). The Lafatsch mine, 47 km by road north of Innsbruck is situated in the "Hinterautal" (Hinterau valley) in the neighborhood of the source of the Isar river in the "Karwendelgebirge" (Karwendel mountains).

3,2 The Lafatsch Mine

The mountain ranges on both sides of the outlet of the Hinterau valley consist of triassic rock (sedimentary rock), primarily of Hauptdolomite, sloping to the south. This formation, being pushed south in the vicinity of the mine, which is further upstream, gives way to older Wetterstein limestone and Raibler strata north of the valley. The Hinterau valley is connected to the "Vompex Loch", a narrow gorge terminating at the village Vomp in the Inn valley, by a wide pass, the "Überschall". In the area of this pass are located numerous mediaeval ore workings. About 4 km west of these workings a development mine, the "Lafatsch mine" has recently been opened in the "Kaston" a flat section of the Hinterau valley at the foot of the "Reps", an eminence in the ridge north

of the Hinterau valley. This mine is worked for lead and zinc. Ores occur as galena (galenite, PbS) and zincblende (ZnS) in pockets and strongly torn tabular-shaped orebodies.

3,3 The Schwaz Mine

The Tuxer Gebirge, consisting of argillaceous slate and striking from west to east exhibits a structure of a highly inhomogeneous nature. On its northern slope is situated the mediaeval mining town Schwaz. Heavy folds and overthrusts have frequently resulted in an inversion of the stratigraphic column. Archaic rocks like phyllite and intrusive gneisses containing siderite are mostly superimposed on recent argillaceous slates which in their turn have been pushed over quartz phyllites (where numerous mines have formerly been worked for iron from siderite ($FeCO_3$) ores). The underlying, more recent palaeozoic and triassic rocks are mostly Schwaz dolomite, new red sandstone and Partnach strata.

The Schwaz dolomite is the rock mostly interspersed with ore occurring as gray copper ore (tetrahedrite). This Schwaz tetrahedrite ($CaMg(CO_3)_2$) is composed primarily of sulfurous copper, silver, and mercury. The mining system which has been constantly extended since it was started in 1409 has a total length of 240 km.

3,4 The St. Gertraudi Mine

Geological conditions in this area are comparable to those prevailing in the Schwaz region. Predominant strata consist of new red sandstone and Schwaz dolomite ("Gertraudi limestone"). Workable baryte ($BaSO_4$) and small quantities of antimonial gray copper ore occur in seams dipping to the east. The working of these deposits also dates back to the middle ages and therefore a number of suitable old undercut galleries are available.

3,5 Determination of the Dielectric Constant of Rock Samples

As has been outlined in the general geological survey, the predominant mountain-building rock types surrounding the field locations are Wetterstein limestone and dolomite which originates from the former by an exchange of calcium carbonate for magnesium carbonate. Hence dolomite differs chemically only little from Wetterstein limestone.

In view of the experiments concerned with the determination of the field strength versus distance dependence of VLF waves it was essential to measure the dielectric constant of these rock types (some other measurements on baryte and other rock samples were being conducted for informative purposes). In measuring ε the capacitive method has proved to be most efficient: a thin plane parallel rock slab was placed as dielectric between two condenser plates with a diameter of 5 cm. The dielectric

constant and the loss angle were measured directly by means of a General Radio bridge (type 716-C) at various frequencies.

The bridge was driven from an RC-generator (Philips GM2317); a low-frequency millivoltmeter (Philips GM6012) was used as a null instrument.

The rock samples were taken from the separate measuring locations. They were cut up in specially designed cutting machines equipped with a diamond blade (diameter 30 cm). When it seemed necessary they were also ground on a plane milling machine constructed by us. As the slabs had to be very thin, no more than a few millimeters, a large portion of the samples cracked already during the cutting process. Furthermore, it was not always possible to produce the slabs with absolutely plane parallel surfaces. Hence the values obtained initially by means of a condenser with metal plates did not show good agreement. In calculating the capacity of such a plate condenser, characterized by $\varepsilon = 15$ and an interelectrode spacing of 0.5 mm filled with a dielectric, an air gap of 0.2 mm causes an error of 40%. Therefore in the following measurements mercury electrodes were used to replace the metal plates. The rock sample was placed on a mercury layer confined by a metal ring, and the upper contact was established in the same manner. Mercury is used with advantage for this purpose, because it approaches the sample very closely, but does not penetrate into the pores and line fissures often occurring in these rock slabs.

Let C_m be the capacity of the condenser in the presence of a dielectric, and C_o its capacity without dielectric,

ε is then given by

$$\varepsilon = \frac{C_m}{C_o} .$$

C_m was determined by the substitution method in order to achieve sufficient accuracy in the measurements. With this method the spurious capacities and the loss factor of the leads can be ignored. The error resulting from neglect of the edge field of the condenser is below the experimental accuracy, as has been shown by theoretical calculations. C_o was either determined by the substitution method or by computation. The dielectric constant and the loss factor were measured in the frequency range extending from 100 c to 100 kc. The curves showing the course taken by these two quantities versus the frequency can be seen in Fig. 3,1. Rock samples were taken from dolomite, Wetterstein limestone and baryte.

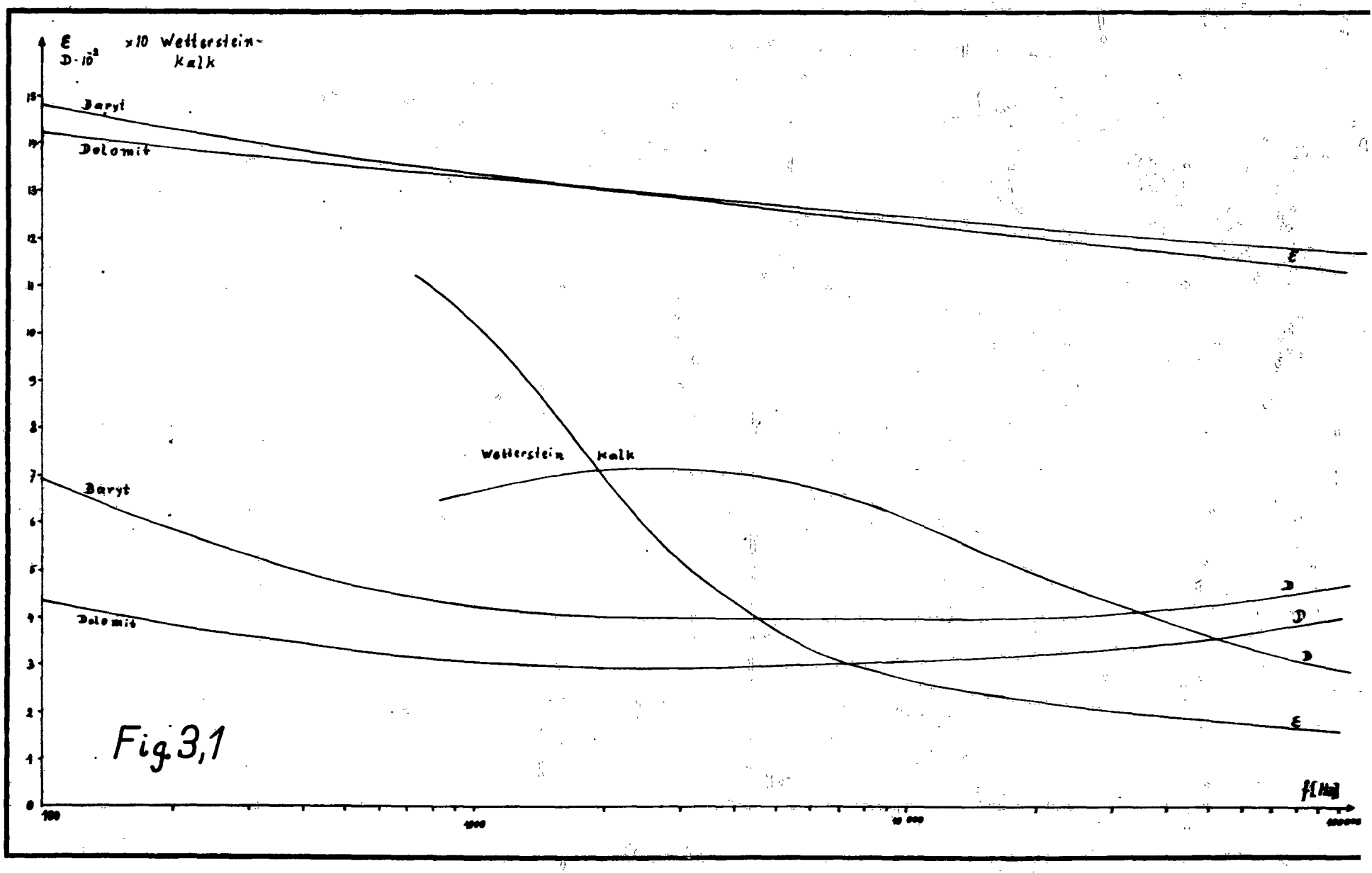
ε
D·10²
x10 Wetterstein-
Kalk
Baryt
Dolomit
Wetterstein Kalk
Baryt
Dolomit
ε
D
D
D
ε
f[Hz]
100
1000
10 000

Fig. 3,1

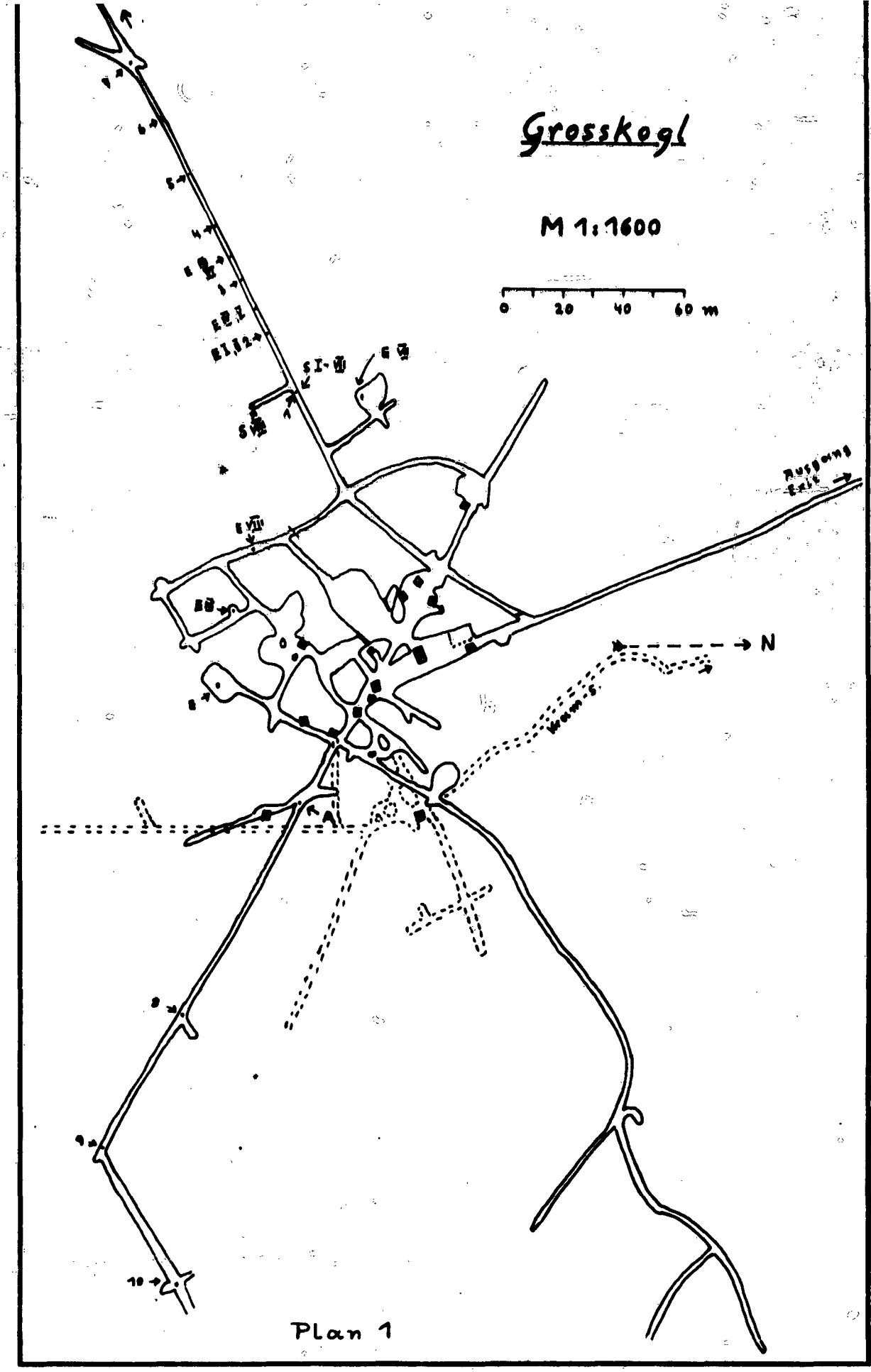

Plan 1

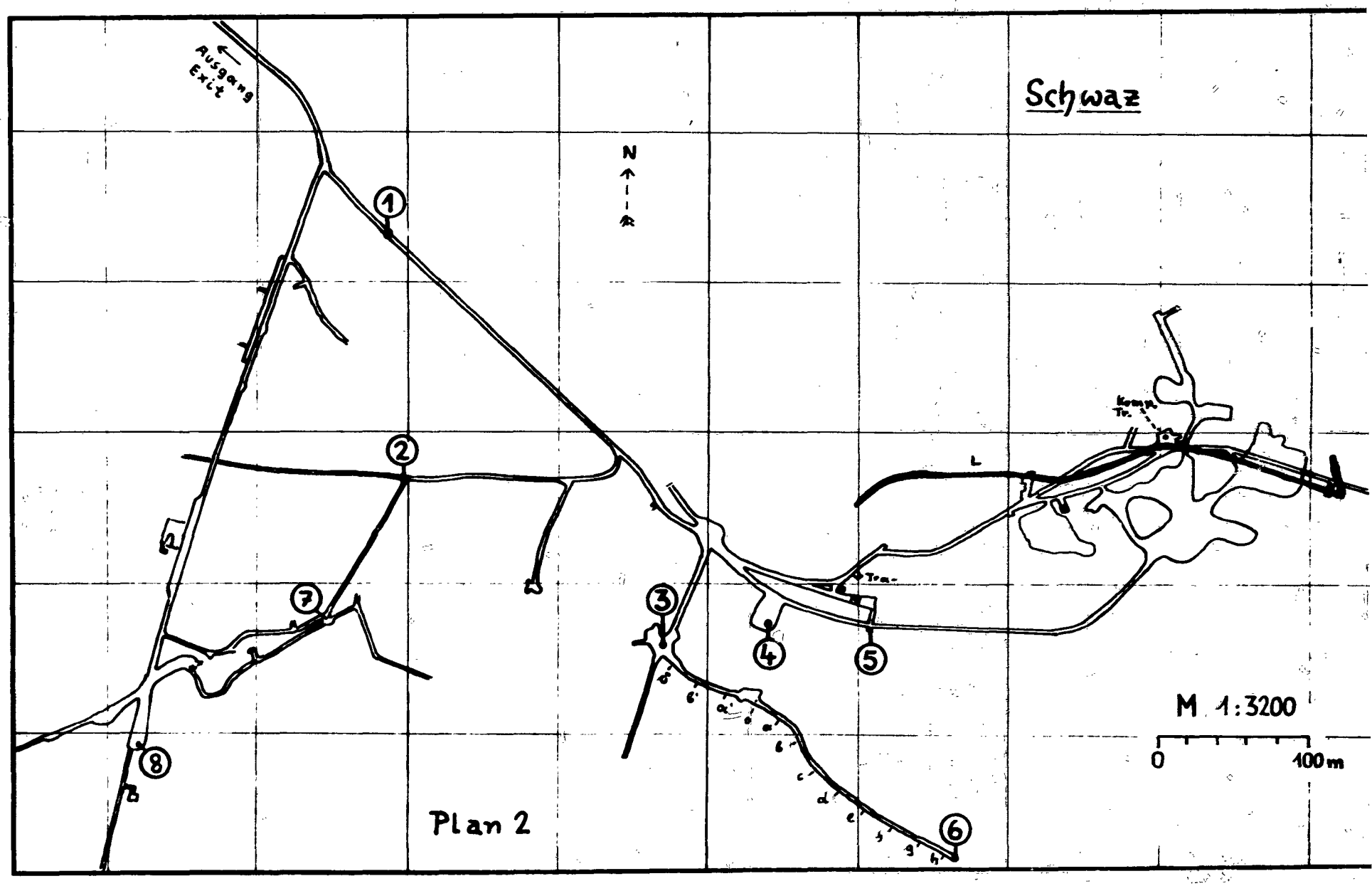
Ausgang
Exit
Schwaz
N
1
2
3
4
5
6
7
8
L
M 1:3200
0
100 m
Plan 2

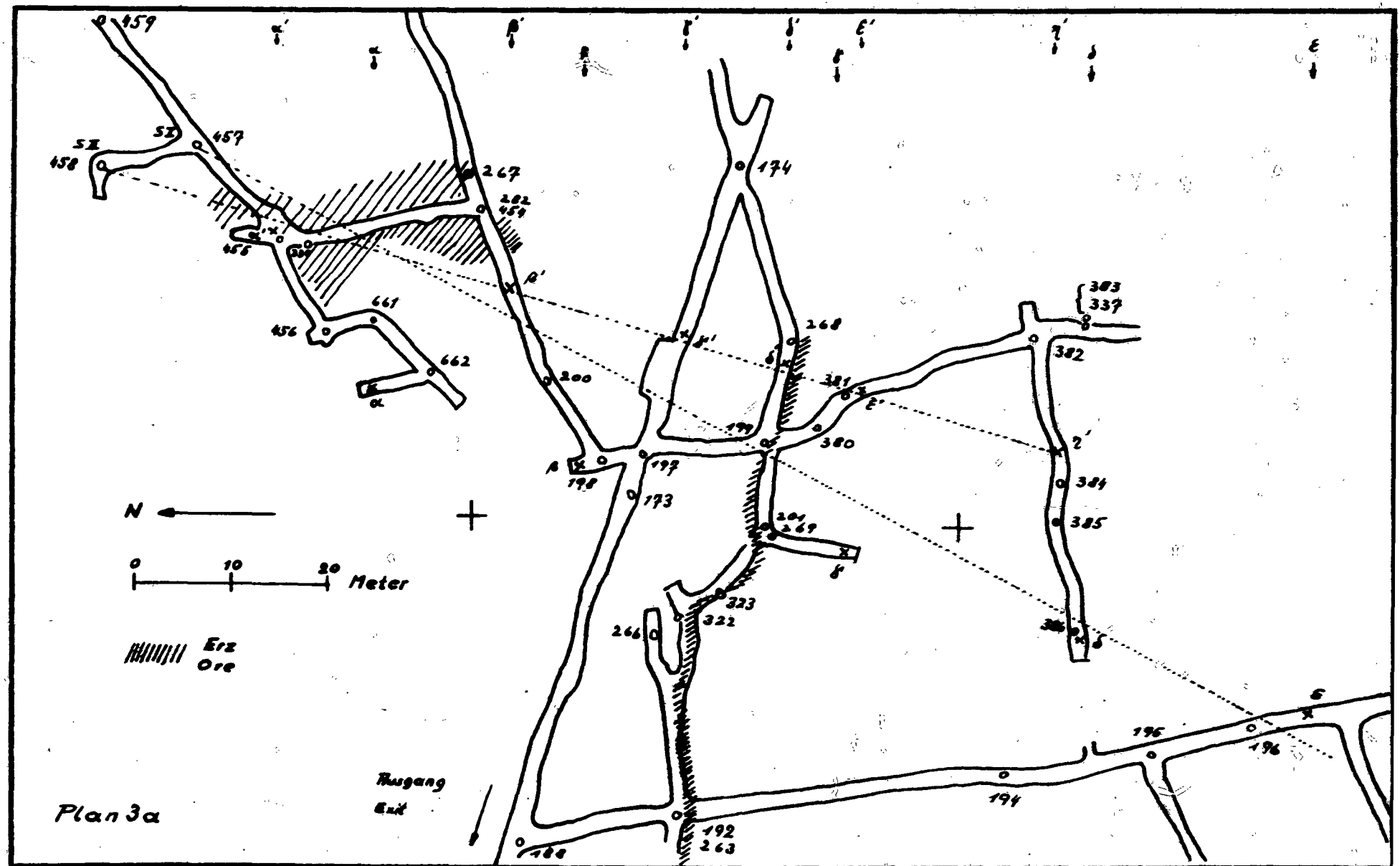
459
457
458
267
282
459
456
661
662
200
174
268
383
337
382
381
380
384
385
201
269
323
322
266
198
197
193
196
194
192
263
N
0
10
20 Meter
Erz
Ore
Ausgang
Exit
Plan 3a

Plan 3b
Plan 3a

fig. I

fig. II

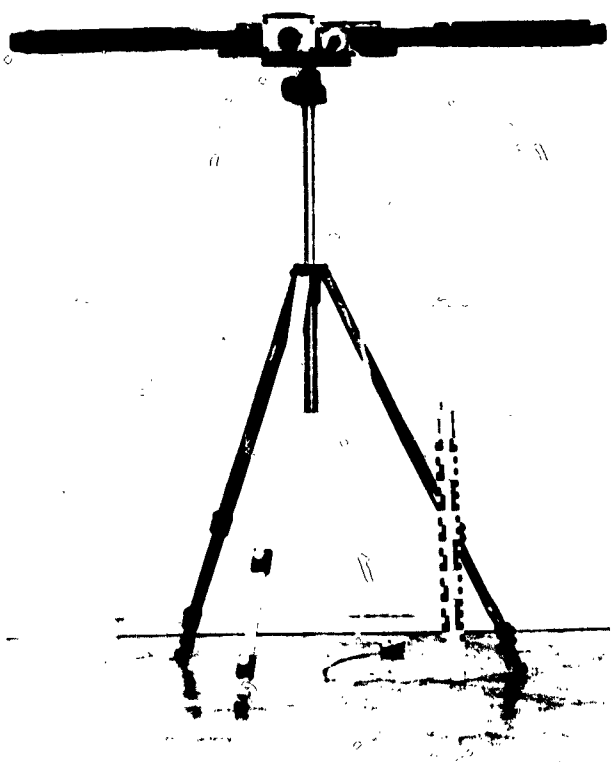

fig. III

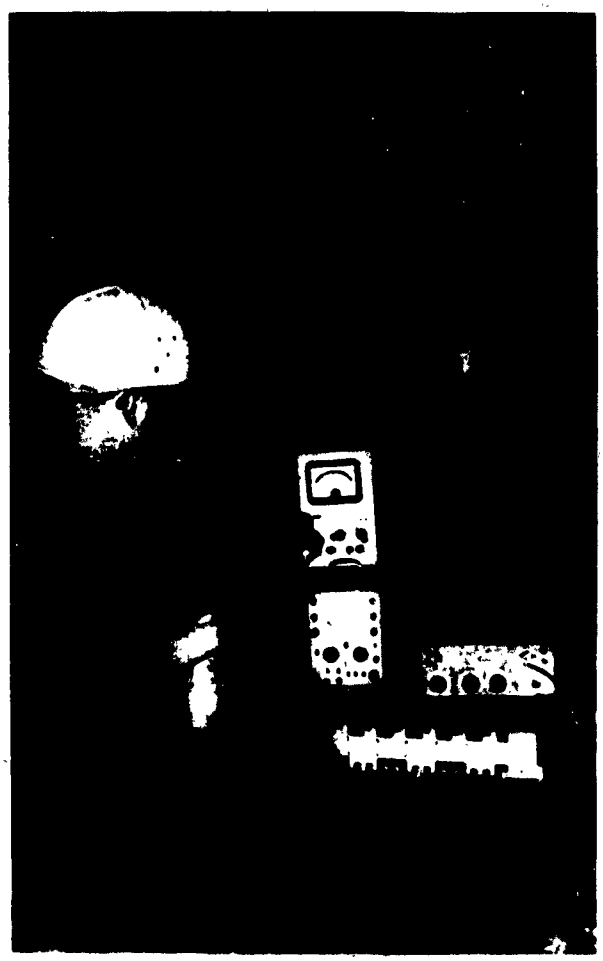

fig. IV

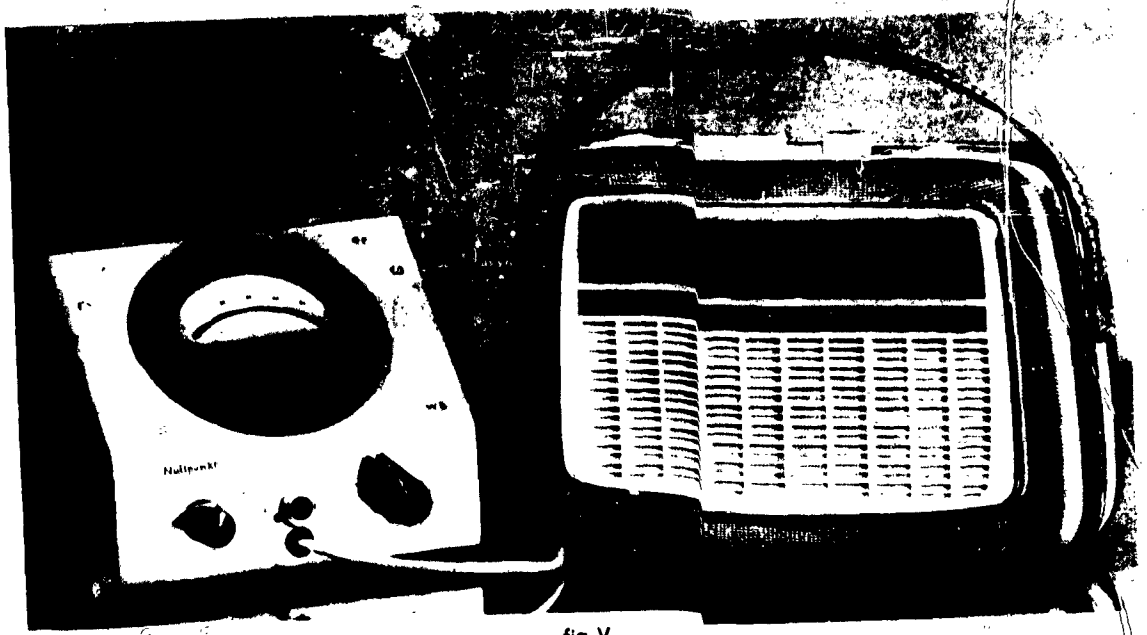

fig. V

fig. VI

fig. VII